Heterogeneous Photocatalysts for Light-Mediated Reversible Deactivation Radical Polymerization

Sarah Freeburne,[b] *Brock Hunter,*[b] *Kirsten Bell,*[b] *Christian W. Pester**[a]

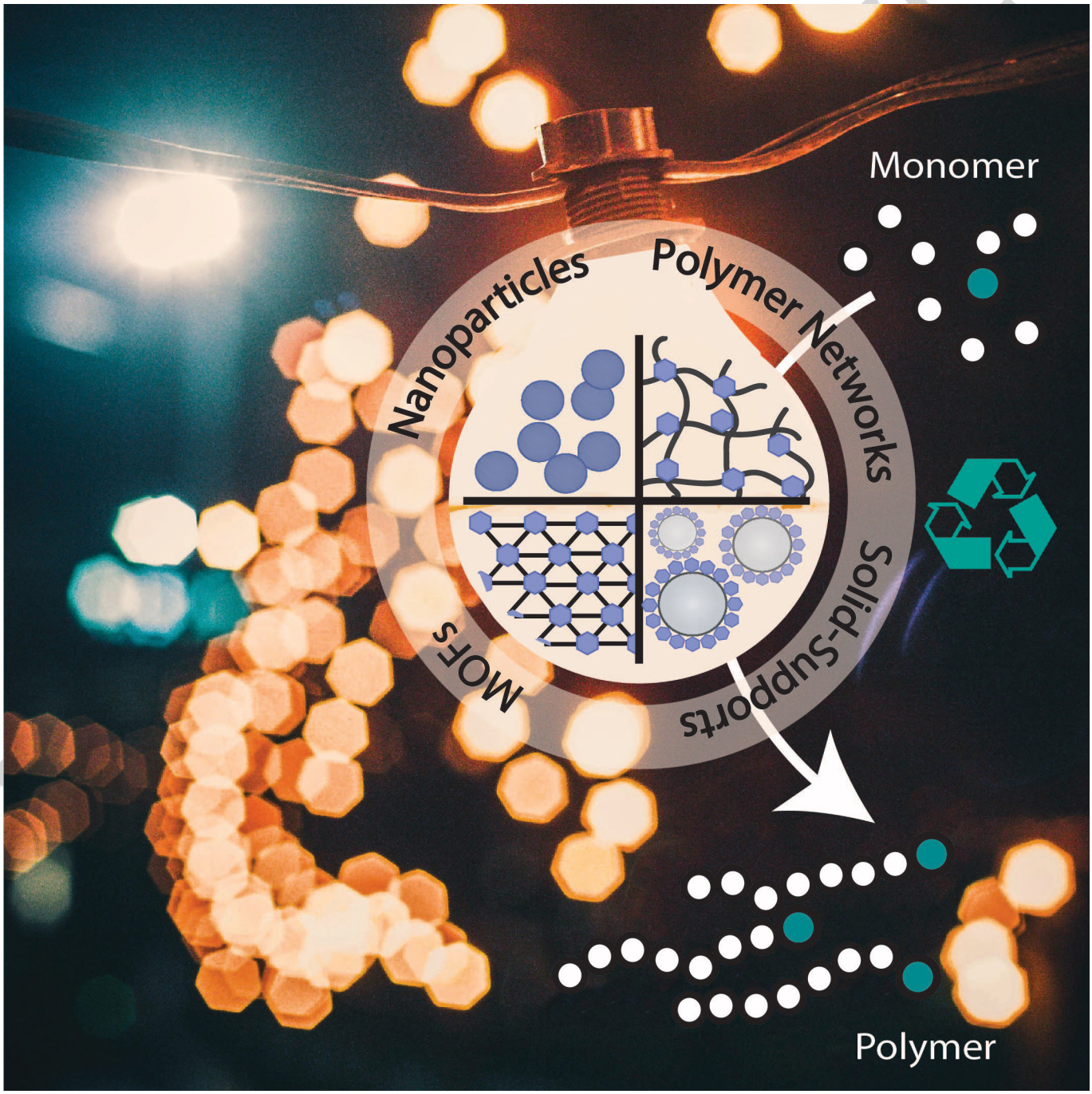

[a] Prof. C.W. Pester
Department of Chemical Engineering,
Department of Materials Science and Engineering,
Department of Chemistry,
The Pennsylvania State University, University Park, Pennsylvania 16802, United States
E-mail: pester@psu.edu

[b] S. Freeburne, B. Hunter, K. Bell
Department of Chemical Engineering, The Pennsylvania State University, University Park, Pennsylvania 16802, United States

Abstract: Heterogeneous photocatalysis combines the benefits of light-mediated chemistry with that of a catalytic platform that facilitates re-use of (often expensive) photocatalysts. This provides significant opportunities towards more economical, sustainable, safe, and user-friendly chemical syntheses of both small and macromolecular compounds. This contribution outlines recent developments in the design of heterogenous photocatalysts and their use to mediate polymerizations. We outline four classes of heterogeneous photocatalysts in detail: nanoparticles, conjugated and non-conjugated polymer networks, metal-organic frameworks (MOFs), and functionalized solid supports.

Sarah Freeburne is currently a 4th year Ph.D. student in the Department of Chemical Engineering at The Pennsylvania State University, where she received the Louis S. and Sara S. Michael Endowed Graduate Fellowship in Engineering. She received her B.S. degree in Chemical Engineering from the University of Kansas in 2019. Her research interests include heterogeneous photocatalysis, reversible deactivation radical polymerization, and reactor engineering.

Brock Hunter is a 1st year Ph.D. student in the Department of Chemical Engineering at The Pennsylvania State University, where he received the University Graduate Fellowship. He received his B.S. degree in Chemical Engineering from Auburn University. His research interests include heterogeneous photocatalysis, polymer brushes, and renewable energy.

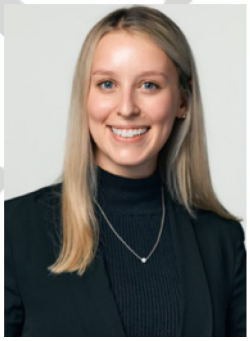

Kirsten Bell recently just defended her Ph.D. thesis in Chemical Engineering at The Pennsylvania State University under the mentorship of Prof. Christian Pester. She will be continuing her research efforts at The Dow Chemical Company. Kirsten received her B.S. in Chemical Engineering from Lehigh University in 2018 with a minor in Business. Her research interests include materials and sustainability.

Prof. Dr. Christian W. Pester is currently the Thomas K. Hepler Early Career Professor in Chemical Engineering at The Pennsylvania State University. Christian received his doctorate *summa cum laude* from the DWI - Leibniz Institute for Interactive Materials (RWTH Aachen University, Germany). From 2014 – 2017 Christian was hosted by Profs. Edward J. Kramer and Craig J. Hawker at the University of California, Santa Barbara (USA) as an Alexander-von-Humboldt Feodor-Lynen Postdoctoral Fellow. Christian is an elected member-at-large of the ACS PMSE division, awardee of the ACS PRF and NSF CAREER awards, and ACS PMSE Young Investigator 2022.

1. Introduction

Researchers in recent years have pushed photochemistry to new frontiers,[1] especially considering an urgent need for increased energy efficiency and safer processing conditions. The sustainability benefits of photocatalysis extend to taking on the challenges of plastic waste, where significant opportunities exist for heterogeneous photocatalysts to make an impact.[2,3]

Photocatalysts (PCs) absorb energy in the form of photons to reach excited states. These may facilitate chemical reactions through either energy or electron transfer. PCs thus lower activation energies for chemical reactions and accelerate the rate of various reactions. In contrast to thermal catalysis, many additional synthetic benefits can be introduced with PCs: wavelength selectivity[4–6] to target specific bonds, temporal control to stop and restart reactions,[7–9] and spatial control to pattern surfaces.[10,11] Together, this affords complex syntheses under low temperatures, ambient pressures, and under a broad range of wavelengths of light – spanning from the ultraviolet (UV) through the visible and into the near infrared range (290–980 nm).[12–16]

However, the PC's desirable strong photon absorption also means that light penetration into the reaction medium is limited by Beer-Lambert's law.[17] PC residuals in the final product can lead to discoloration and their excited states can promote degradation.[18–20] Finally, the high cost of transition metal PCs and often-complex syntheses for organic alternatives further limit their use on large scales. These, amongst other challenges, motivated the development and study of heterogeneous photocatalysts.[21–25]

Because heterogeneous PCs are, by definition, in a different phase than the reactants (e.g., solid PC in liquid medium), opportunities arise to facilitate catalyst separation from the reaction mixture by e.g., filtration,[26] centrifugation,[27] or externally applied force fields (e.g., magnetic recovery).[28,29] This reduces waste, mitigates catalyst contamination, and provides economic benefits by allowing reuse of the (potentially expensive)[30,31] catalysts. Furthermore, many creative opportunities for scale up have been suggested, such as continuous flow systems, which may operate with heterogeneous PCs as packed beds and could potentially remove the need for a catalyst separation processing step and recovery altogether.[32–36]

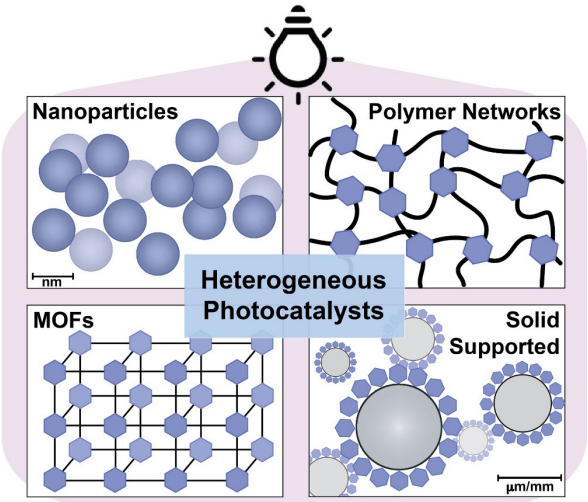

Figure 1. Illustration of different heterogeneous photocatalyst categories that will be discussed in this article: (i) nanoparticles, (ii) polymer networks, (iii) metal-organic frameworks (MOFs), and (iv) solid supported photocatalysts.

Despite these exciting opportunities, challenges remain that warrant, and require, further investigation. Our objective with this contribution is to discuss four major classes of heterogeneous PCs: (i) nanoparticles, (ii) polymer networks, (iii) metal-organic frameworks (MOFs), and (iv) solid supported PCs (see **Figure 1**). A particular focus will be placed on their use in reversible deactivation radical polymerization (RDRP), for which we intend to outline their individual benefits and limitations. As our focus lies on polymerizations, we refer the reader to other comprehensive surveys on heterogeneous PCs for small molecule reactions and other, more specialized, applications.[37–39]

Light-mediated Radical Polymerization

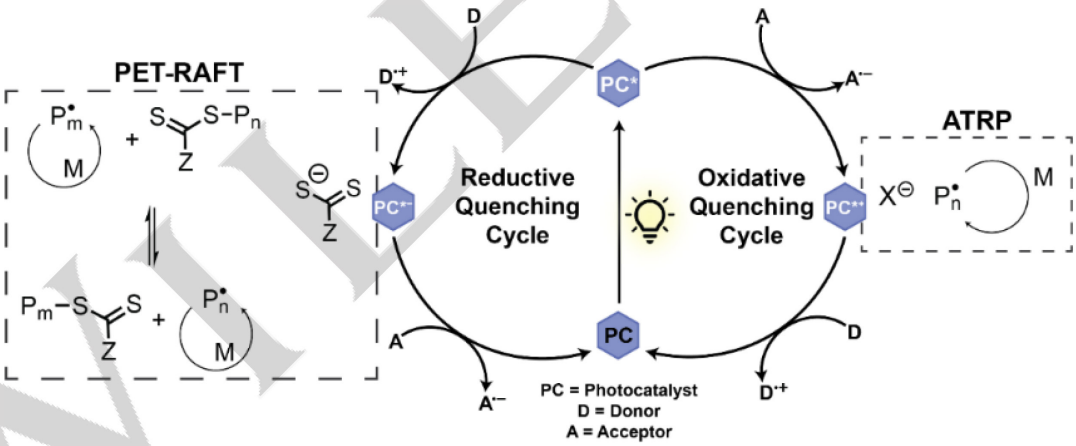

Figure 2. General example mechanisms for Photo-induced Electron Transfer Reversible Addition Fragmentation Chain Transfer (PET-RAFT) polymerization (left). A photocatalyst (PC) absorbs light energy to reach an excited state, and then accepts an electron from an electron donor (D), to become a radical anion, from there, interaction with the RAFT CTA results in a propagating radical which can add monomers (M) to form a polymer (P_m) via the RAFT equilibrium. Light-mediated Atom Transfer Radical Polymerization (right) is displayed as an oxidative quenching cycle, where a PC in the excited state transfers an electron to an electron acceptor (A), and the cationic PC forms a complex with a negatively charged halogen (X^-). ATRP polymerization may occur, until an electron donor (D) reduces the PC back down to its ground state. Please note the example mechanisms are not all encompassing.

Photocatalysis has become an increasingly effective means to synthesize well-defined polymers in solution[40] and from surfaces.[41–48] Beyond conventional radical photoinitiation,[49,50] significant advances have been made in *mediating* polymerizations. This now allows the use of milder visible and (near) infrared wavelengths (vs. UV initiation) to stop and (re)start polymerizations by toggling the light source off and on. The resulting materials exhibit precise molecular weights, low molecular weight distributions ($Đ$ < 1.5), and retained chain ends to afford access to complex architectures (e.g., block copolymers,[51,52] star polymers,[53] bottle brushes,[54] surface-grafted polymers,[41,42,44,55,56] etc.). Because photocatalysts require a particular wavelength for activation, chromatic orthogonality may be achieved and disparate reactions may

be performed in one pot using different catalysts or wavelengths.[57–59] Ionic,[60,61] metathesis,[62,63] ring opening,[64,65] different step-growth polymerizations,[66–69] and various reversible-deactivation radical polymerizations (RDRP)[40,70,71] can now be mediated by visible light with excellent spatiotemporal control. A majority of research has focused on the latter, with light-mediated RDRP techniques including but not limited to: Atom Transfer Radical Polymerization (ATRP),[72–75] Photo-induced Electron Transfer-Reversible Addition-Fragmentation Chain Transfer polymerization (PET-RAFT),[41,76,77] Nitroxide Mediated Polymerization (NMP),[78,79] and photo-iniferter polymerization.[80,81]

More specifically, ATRP polymerization (see **Figure 2**, right) occurs via activation of an alkyl halide initiator, i.e., the excited state PC transfers an electron to the alkyl halide (oxidizing the catalyst) and the halogen is removed.[74,86] Chain growth then proceeds from the formed radical until the halogen/PC pair encounters a propagating chain again. By returning the growing active chain into its halogenated (dormant) state, the PC is reduced to its ground state and this cycle can be repeated. Notably, reductive quenching mechanisms are also feasible for ATRP through addition of sacrificial reductants.[87]

PET-RAFT polymerizations can proceed through oxidative quenching pathways or via energy transfer from a photocatalyst in its triplet excited state (see **Figure 2,** left).[77,87–89] PET-RAFT polymerization employs thiocarbonylthio-derivatives as chain transfer agents (CTAs) which can undergo the well-established RAFT equilibrium to mediate polymerization. Deactivation occurs upon collision between the radical cationic photocatalyst, the anionic RAFT agent, and a radical propagating chain, but various groups are still studying this mechanism in more detail.[90–92]

Photocatalyst Requirements

Given the above mechanistic considerations, important requirements arise that qualify an effective photocatalyst: (i) efficient photon absorption, (ii) excited states of sufficient energy to drive the targeted chemical reactions, and (iii) adequately long excited state lifetimes to enable electron or energy transfer between the catalyst and substrate.[87,93]

The molar absorption coefficient, ε, describes the ability of molecules to absorb light and can vary on the solvent being used. Generally, ε values range from on the order above 50,000 $M^{-1}cm^{-1}$ to 1,000 $M^{-1}cm^{-1}$.[94,95] While strong absorption is favorable for efficient photon absorption of the PC, this also reduces light penetration into the reaction medium, as described by Beer Lambert's law, and limits scalability. The wavelength of maximum absorption, λ_{max}, can be targeted specifically by narrow emission LED light sources. PCs with longer λ_{max} are preferred to reduce possible side reactions, but values within the UV range are still of interest.

The excited states of the PCs need to be sufficiently long-lived to allow energy/electron transfer processes to occur with reagents. Excited state lifetimes of PCs can be on the order of nanoseconds (e.g., 4.2 ns for fluorescein), or microseconds (e.g., 2.4 μs for Rose Bengal^{2-}).[82] Generally, longer lifetimes have been shown to improve photocatalytic ability in many synthetic transformations[96] and polymerizations.[97] Recent research into prolonging lifetimes may enable new approaches by leveraging e.g., delayed fluorescence.[98] Such delayed fluorescence catalysts indeed have allowed for successful polymerizations of fluoroalkenes.[99]

Mechanistic Considerations

Various in-depth and comprehensive reviews[16,82–84] on the photophysics of photoredox catalysts exist. Here, we wish to briefly summarize some important concepts. Photocatalytic processes generally begin by absorption of photons. The resulting excited state of the PC may then donate (oxidative quenching) or accept an electron (reductive quenching). Subsequently, the catalyst is returned to its ground state and the PC may begin another catalytic cycle. If the excited state PC transfers energy (rather than an electron) this process is referred to as photosensitization.[85]

The energetic potential of an active state to drive reactions is often expressed in terms of its oxidation or reduction potential. For a specific target reaction, an appropriate PC with sufficient potential must be chosen. For light-mediated polymerizations (ATRP, RAFT, etc.), it is important to match the required potential of the PCs with the energy required to activate the initiators (or chain transfer agents). As an example for ATRP using ethyl α-bromophenylacetate (EBP) initiators, the PC's oxidation potential must be high enough to meet EBP's reduction potential (-0.74 V vs. SCE).[87,100]

Many transition metal complexes based on ruthenium (Ru),[101] iridium (Ir),[102,103] and zinc (Zn)[104] meet these energetic requirements and have demonstrated high efficacy in photocatalysis. Ir- and Ru-based catalysts combine the benefits of long-lived excited states and high reduction potentials. *Fac*-tris[2-phenylpyridinato-C^2,*N*]iridium(III), (*fac*-$Ir(ppy)_3$) ligand modification offers tuning of absorption or reduction/oxidation properties.[94,105] A less expensive, but effective alternative is tris(2,2'-bipyridine)ruthenium(II), $Ru[bpy_3]^{2+}$.[106] Excited state lifetimes are ca. ~550-2500 ns for Ir-based catalysts[94] and ca. 500-1000 ns for $Ru[bpy_3]^{2+}$.[83] Reduction potentials have been reported as $E_{1/2}^{red} = -2.17\ vs\ SCE$[107] for *fac*-$Ir(ppy)_3$ and $E_{1/2}^{red} = -0.72\ vs\ SCE$ for $Ru[bpy]_3^{2+}$.[108] For ATRP, this means *fac*-$Ir(ppy)_3$'s excited state is reducing enough to create the EBP initiator's carbon-centered radical that is required for polymerization. The removed bromine complexes with the $Ir(ppy)_3$ catalyst's radical cation. The newly formed $[Br^-/Ir(ppy)_3^{\bullet/+}]$ complex has a reduction potential of 0.77 V while anionic EBP has a reduction potential of -0.74 V. This is important because the active chain end can return an electron to the highly oxidizing $[Br^-/Ir(ppy)_3^{\bullet/+}]$ complex, returning $Ir(ppy)_3^{\bullet/+}$ to its ground state. Simultaneously, the polymer chain is returned to the dormant state as the bromine bonds with the radical chain end, and the cycle may repeat itself.[87,100]

While transition metal-based catalysts offer high efficacy, high cost and metal contamination from their degradation remain a significant concern in their widespread adoption.[94,109] Organic catalysts are a desirable alternative as they offer similar abilities and are generally less expensive.[16,110] Many of the reported and readily available organic photocatalysts are based on xanthene dyes and their derivatives. Examples include Rose Bengal,[111] fluorescein,[112] erythrosine B,[113] and Eosin Y.[16,114–116] However, unlike transition metal complexes, xanthene dye photocatalysts often require the addition of tertiary amines such as triethylamine (TEA). Evidence exists to suggest that tertiary amines assist in the polymerization process by acting as a sacrificial electron donor,

able to transfer an electron to the catalyst. This is thought to result in the PC acting in accordance with the reductive quenching mechanism. The utility of tertiary amines is shown for PET-RAFT polymerizations[117,118] as well as ATRP.[119]

Excitingly, xanthene dyes may be modified to be activated by mild near-IR wavelengths.[120] However, many xanthene dyes are highly colored, and therefore there is also much interest in the photocatalytic degradation of these catalysts themselves as they may result in undesirable staining of products.[18,121] This again highlights the motivation behind using them as heterogeneous photocatalysts to facilitate their removal after the reaction. Phenoxazine-[122], phenothiazine-[123–125], and phenazine-derivatives[126] have also been studied extensively and are good examples of how chemical modification of a catalytic core can influence photocatalytic properties (e.g., shifting absorption and increasing reduction potential). For example, for phenothiazine derivatives, investigations have determined that electron withdrawing groups can lower the excited state reduction potential.[127] Highlighting the impact of such modifications for RDRP performance, Treat et. al. compared 10-methylphenothiazine to 10-phenylphenothiazine and found lower dispersity for poly(methyl methacrylate) polymers synthesized via ATRP.[128] Dispersity improved from $Đ$ =1.74 to $Đ$ =1.30 when an electron donating methyl group on the PC was changed to an electron withdrawing aromatic group. These design principles have proven useful for computer-aided design strategies, which have allowed the discovery of effective catalysts at 0.5 ppm catalyst loadings for ATRP.[129] Finally, another major class of organic photocatalysts is that of carbon nitrides, also including graphitic carbon nitrides.[130,131] It is notable that both Eosin Y and carbon nitrides have demonstrated catalytic ability in depolymerization[132] and catalytic oxidation of polystyrene,[133]– suggesting great potential in their future use in a circular plastic economy. Both organic and organometallic catalysts are generally able retain catalytic ability when modified with functional groups.

Catalyst stability is a major consideration as photocatalysts can degrade (often referred to as photobleaching) over time and under exposure to light.[18,134,135] Photobleaching may occur via different pathways, some that are dependent on oxygen and others that result from autocatalysis.[135,136] Another consideration for catalyst selection are quantum yields. Quantum yields are often not reported for photocatalysts and thus it is often difficult to compare catalytic efficacy. Generally, heterogeneous PCs feature complex 3D geometries and macroscopic catalyst dimensions can make it challenging to characterize these systems. However, some techniques have been proven useful. For nanoparticle systems, UV-Vis spectroscopy and fluorometry may be used with suspended particles. For other PCs, solid-state techniques can be leveraged, such as diffuse reflectance spectroscopy, which may assist in determining optical properties. For many examples, it is often uncertain if the catalyst concentration is optimized, which is significant because catalyst efficacy may appear lower depending on the concentration used.[137] Catalyst properties such as molar absorption coefficients and redox potentials are often studied in isolation with the catalyst and solvent, and therefore unforeseen side reactions leading to photobleaching and catalyst deactivation are not captured.[31,138]

A note of relevance for photocatalysis is the role of oxygen. Oxygen (added or environmental) may be useful in photosensitized systems,[139] but is generally undesirable in photocatalytic systems where radical intermediates are key and electron transfer occurs.[140] Various strategies have been developed to mitigate the effects of ambient oxygen in RDRP.[141] Examples include the light-mediated generation of reactive singlet oxygen through chemical reactions $^1O_2$ can react with the solvent (e.g., DMSO),[141] with additives (e.g., 9,10-dimethylanthracene),[142] or with a (co)-monomer itself (e.g., 2-(methylthio)ethyl methacrylate).[143] Other strategies include the consumption of ambient O_2 by enzymes, such as glucose oxidase (GOx), to generate hydrogen peroxide.[144–146] Reducing agents, such as ascorbic acid, may regenerate an oxidized catalyst, as is the case for copper catalysts in activators regenerated by electron transfer (ARGET) ATRP.[73] There is evidence that tertiary amines may also increase the oxygen tolerance of these systems.[130] The addition of tertiary amines (e.g., TEA) shortens induction periods and increases polymerization rates. This results from the ability of tertiary amines to act as sacrificial electron donors to generate anionic PCs, which are then able to reduce oxygen.[117] Some photocatalysts that require oxygen as a cocatalyst have also been discovered.[147] Oxygen tolerance is a highly desirable feature as purging steps require additional infrastructure.

It becomes evident that it is possible to modify various photocatalysts with functional groups that also allow tethering to solid supports and heterogenization. In the following, we will discuss and explore four major categories of heterogeneous photocatalysts for polymerizations: (i) nanoparticles, (ii) polymer gels/networks, (iii) metal organic frameworks (MOFs), and (iv) solid-supported catalysts. These categories are not intended to be mutually exclusive, nor are they intended to be all-encompassing, but a representative reflection of the major categories seen in photo-RDRP literature.

2. Nanoparticle Photocatalysts

Both inorganic and organic nanoparticles have been successfully used for a plethora of organic photocatalytic reactions.[148–151] Their small size and large surface to volume ratio improves accessibility for reactants while also providing opportunities for recovery through e.g., centrifugation.

Inorganic Nanoparticles

Many early reports in heterogeneous photocatalysis were focused on inorganic (metals or metal oxide) nanoparticles or quantum dots (semiconductor nanocrystals). Seminal reports were primarily focused on the use of titanium dioxide (or titania, TiO_2)[12,152] and its use for the photolysis of water.[24,153,154] These studies leveraged TiO_2's ability to act as a photosensitizer for generation of active oxygen species, which can degrade pollutants in wastewater[155,156] or catalyze plastic degradation.[157,158] For photocatalysis to occur in semiconductors, electron-hole pairs are generated by promoting electrons to the conduction bands by absorbing photons of sufficient energy to cross the material's band gap.[159] This band gap can be modified, e.g., by adding defects like oxygen vacancies to reduce TiO_2's E_{gap}.[160] Once generated, both electrons and holes can migrate to the TiO_2 surface through movement in the valence and conduction bands, where they are then useful to drive reactions.

Both catalyst and synthetic scope have since been significantly broadened. Various nanomaterials have shown great efficacy as heterogeneous photocatalysts in suspended[161] or surface-

immobilized form[159,162,163] for organic synthesis,[164] RDRP,[29,165–167] or degradation of contaminants.[148] Examples include metals (e.g., gold,[168] silver,[168] copper, etc.),[43,169] metal oxides (e.g., zinc-[170] and copper oxides[171,172]), and semiconducting nanoparticles (e.g., cadmium selenide, CdSe[173,174]).

Both metal oxides and semiconductor nanoparticles, e.g., silica and titania, have also proven useful for RDRP. Silica supports for silica quantum dots, for example, have been successful photocatalysts for ATRP.[175] Studies also highlight the efficacy of other (modified) metal oxides. As Dadashi-Silab et. al. found, the incorporation of Fe into ZnO nanoparticles can improve photocatalytic performance.[176] Fe-doped ZnO increased the rate of polymerization and monomer conversion increased from 40% to 57% over the course of 3 hours in 350 nm light for methyl methacrylate while also decreasing the final dispersity from $Đ$ =1.23 to $Đ$ =1.18.

In contrast to UV-absorbing TiO_2 and other metal oxides, metal nanoparticles (e.g., gold) are able to absorb light in the visible region and have been useful for a variety of chemical transformations.[177] Moreover, some photocatalysts feature enhanced absorption capabilities through localized surface plasmon resonance (LSPR).[178] When the oscillation frequency of the incident light and electrons in the catalyst match, constructive interference occurs and a strong absorption peak is observed. Au and Ag are examples of catalysts with this LSPR effect.[177,179] While to the best of our knowledge, metal nanoparticles such as gold, copper, or silver have not yet been utilized for RDRP, semiconductors such as silica and titania are widely used as support materials for metal catalysts. For example, titania can be implemented as a support for silver,[43] immobilized gold is capable of variety of photooxidations of aromatic alcohols,[180] solid-supported and ZnO can be used for water photolysis and dye degradation.[181]

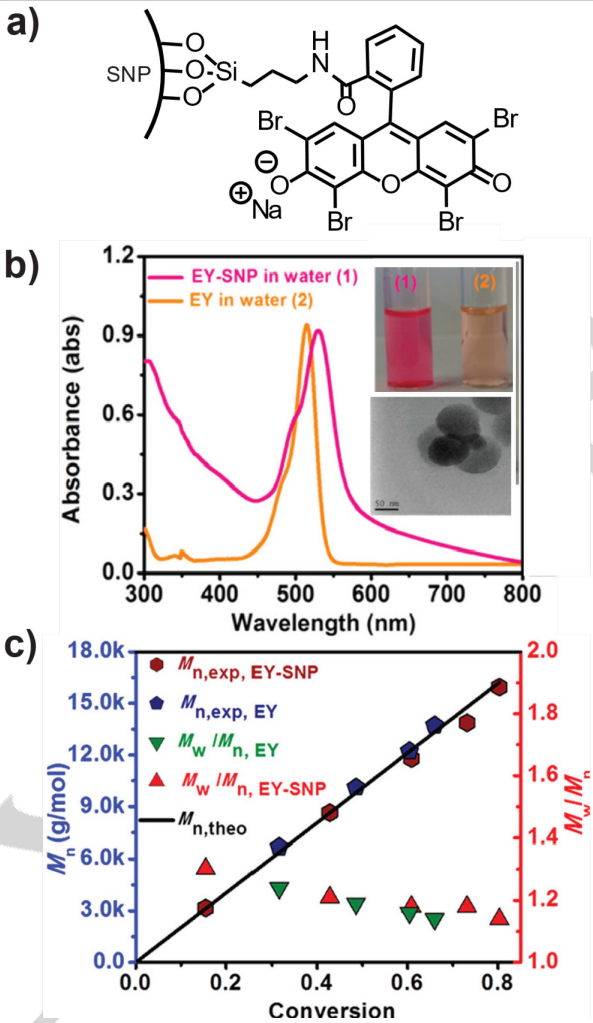

Figure 3. a) Schematic of Eosin Y grafted to silica nanoparticles (EY-SNP). b) UV-Vis spectra of EY-SNP and Eosin Y in water with transmission electron micrographs of the SNP-EY nanoparticles (inset, scale bar is 50 nm). c) Kinetics and evolution of dispersity during dimethyl acrylamide PET-RAFT polymerization in water (in the absence of oxygen and at room temperature). Reproduced from ref. [166] Copyright (2018), with permission from American Chemical Society.

While pure metals and metal oxides have not yet demonstrated much use for RDRP, perovskites have been shown to be effective. This includes perovskites in conjunction with lead halide nanocrystals, ($CsPbBr_3$) which may be used to catalyze PET-RAFT polymerizations.[182] The perovskites were able to function under blue LED lights, or under 800 nm laser pulses, indicating versatility in reaction conditions. However, recycling experiments were not reported for the perovskite nanocrystals so their longevity remains unclear.

CdSe quantum dots, modified with mercaptopropionic acid (MPA), were also shown to efficiently catalyze PET-RAFT polymerization in aqueous environments. McClelland et al. described 81% conversion of dimethylacrylamide (DMA) in 2 hours to provide well-controlled macromolecular materials ($Đ$ = 1.01, M_n = 19,200 g/mol) at a catalyst loading of 0.43 ppm under green laser irradiation (532 nm, 40 mW/cm^2).[165] The authors showed recovery of MPA-CdSe quantum dots through centrifugation and their photocatalytic performance was maintained over four reaction cycles. A 5.5% decline in conversion and an increase in dispersity of 0.04 was observed, but the 5th use cycle showed a more significant decrease in conversion (-29.5%) and dispersity increased

markedly (*Đ* = 1.20). Beyond this limited lifetime, the final polymer product also showed 8.41 µg/g of cadmium contamination – pointing towards practical limitations of centrifugation as a separation method.

Despite their high photostability,[183] limitations of inorganic nanoparticles have motivated researchers to examine alternatives. Limitations include (i) inferior colloidal stability in common organic reaction solvents,[184] (ii) high visible light absorption that significantly reduces scalability, (iii) possible electron-hole recombination, which decreases catalyst efficiency,[177] and (iv) a highly material-specific band gap which limits opportunities to modify catalyst selectivity.

Organic Nanoparticles

Inorganic/organic hybrid[185] and fully organic nanoparticles[186] have been studied to improve light penetration and reagent affinity towards the nanoparticle surface.[43,187] Organic nanoparticles can also offer biocompatibility, which can reduce human and environmental hazards known for metal nanoparticles.[188] Finally, the modular nature of organic nanoparticles can afford complex structures that provide opportunities to tailor highly specific reaction sites with modified band gaps.[189]

Nanoparticle agglomeration is a concern that can limit efficacy, but approaches exist to mitigate these concerns. For example, nanoparticle dispersions may be stabilized through surface-tethered polymer brushes. Kim et al. synthesized photocatalytic conjugated microporous polymer (CMP) nanoparticles that were stabilized via poly(methyl methacrylate) and poly(dimethyl acrylamide) polymer brushes.[190] The catalysts could be recycled five times for an oxidative [3+2] cycloaddition reaction with a drop in yield from 69% to 54%. This reduction was attributed to the loss of catalyst nanoparticles over 22 cycles of centrifugation.

Surface-functionalized Inorganic Nanoparticles

Surface-modification of nanoparticles with organic photocatalysts can combine the benefits of organic photocatalyst scaffolds (e.g., tunable photophysical properties) with those of a passive solid-support material (e.g., improved catalyst recovery). Furthermore, studies have suggested that surface-immobilizing organic/organometallic photocatalysts to passive solid supports can also decrease photobleaching and increase their lifetime.[191–193] As an example for this class of materials, Shanmugam et al. grafted Eosin Y to silica nanoparticles and studied their efficacy as PET-RAFT polymerization catalysts (see **Figure 3 & Table 1**).[166] Controlled polymerization of various acrylate monomers was achieved with high recyclability. For the monomer dimethylacrylamide, 66% conversion was reached in 4 hours with good control over dispersity (*Đ* = 1.10, M_n = 13,400 g/mol) at 3 ppm catalyst loading and under green light irradiation (λ_{max} = 515 nm). The Eosin-Y@SiO_2 nanoparticles could be reused five times after purification by centrifugation and limited catalyst degradation was observed. Each reuse showed similar monomer conversions of *n*-butyl acrylate (70-75%) and no appreciable change in dispersity was observed. In contrast, Eosin Y as a small molecule homogeneous catalyst rapidly degraded within 9 hours of polymerization time, suggesting the Eosin-Y@SiO_2 platform provided an increased resistance towards photobleaching after surface-immobilization.

Surface-modifying functional nanomaterials with photocatalysts also allows leveraging synergistic photophysical effects. For example, studies have shown that nanoparticles can perform photon upconversion, i.e., the conversion of low energy light (e.g., (near) infrared, (N)IR radiation) to higher energy light.[194] This light of higher energy can subsequently be used to excite another photocatalyst. This broadening of the usable spectral region for photocatalysis towards longer wavelengths is desirable because it provides the potential to improve scalability by penetrating deeper into the reaction medium.

Photon upconversion may occur via three different approaches: luminescent solar concentrators, lanthanide^{3+} systems, or triplet-triplet annihilation.[195] A detailed elaboration on approaches and mechanisms is beyond the scope of this review, but we refer the reader to an article by Richards et. al.[195] Lanthanide systems have found success for RDRP polymerizations in heterogeneous settings. The approach employs sodium yttrium fluoride as a host, and lanthanide ions (typically) Yb^{3+} and Er^{3+} (other emitter ions include thulium (Tm^{3+}) or holmium ions (Ho^{3+})) for the absorption and emission of light. [195] Typically, Yb^{3+} is chosen as the absorber, as it has a maximum absorbance in the NIR region, λ_{max} = 980 nm.[195] When excited by NIR light, Yb^{3+} may transfer energy to an emitter, Er^{3+}, which may be promoted to a further excited state by another excited Yb^{3+} ion. The emitter is then able to emit light, which is subsequently able to activate a photocatalyst, which will absorb the higher energy light released.[195] This approach has been used for RAFT polymerization, where the $NaYF_4$:Yb^{3+},Tm^{3+} upconverting nanoparticles activated the RAFT agents themselves by emitting blue light.[196] In contrast, Zhang et. al. leveraged a photon upconversion strategy by using β-$NaYF_4$: 30% Yb^{3+}, 1% Tm^{3+} modified silica nanoparticles to conduct ATRP (see **Figure 4 & Table 1**).[15] Under λ_{max} = 980 nm irradiation for 24 hours, low dispersity (*Đ* ≤ 1.28) was achieved for various acrylates and methacrylates – albeit at varying conversions and molecular weights (13-67%, M_n = 3,000 - 36,600 g/mol). The upconversion nanomaterials showed the ability to be reused for 5 cycles. The authors illustrated the benefits of using NIR to penetrate various materials by placing a physical barrier (pig skin) between the reaction vessel and the light source. With this setup, 88% methyl acrylate conversion (*Đ* = 1.16) was achieved in 36 hours. Another approach utilized β-$NaYF_4$:30%Yb/0.5%Tm nanoparticles doped with carbon dots comprised of o-phenylenediamine as a photocatalyst to activate copper catalysts for ATRP.[197]

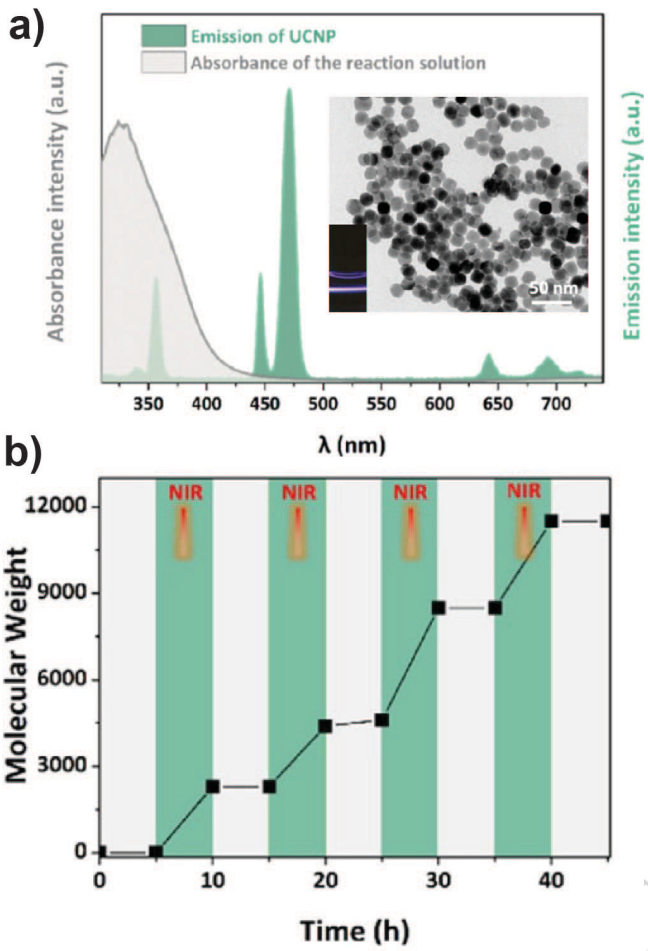

Figure 4. a) Absorbance spectra comparing the emission of the upconverting β-$NaYF_4$: 30% Yb^{3+}, 1% Tm^{3+} nanoparticles versus the absorbance of the polymerization solution. The insert shows a transmission electron micrograph of the nanoparticles with 980 nm laser excitation of the dispersed nanoparticles in dimethyl sulfoxide. b) Temporal control (molecular weight as a function of time) for NIR photo-ATRP of methyl acrylate using upconverting nanoparticles. Reproduced from ref. [15] Copyright (2020), with permission from American Chemical Society.

Outlook for Nanoparticles

In conclusion, initial limitations of titania and other metal/metal oxide nanoparticles included a fixed band gap, electron hole recombination, limited absorption wavelengths, and limited affinity of organic reagents to the surface of inorganic nanoparticles. However, these limitations can be mitigated by combining catalysts or using one catalyst to support another.[198] To this end, Sarina et al. synthesized Au-Pd alloys and found they enhanced the yield for Suzuki-Miyaura cross coupling, the oxidation of aromatic alcohols, and other reactions greatly.[187] Pd showed a strong affinity for organics that Au lacked, so combining the two allowed enhanced performance. For RDRP, a similar effect was found through the combination of iron (Fe) and zinc oxide nanoparticles.[176] Finally, expanding nanoparticles' utility further into the (near) infrared and leveraging photon upconversion strategies may prove a fruitful future direction to further improve light utilization.

Despite their clear potential, more effective methods to efficiently separate nanoparticle photocatalysts from the reaction mixture are necessary. Many nanoparticle photocatalysts (e.g., CdSe) are toxic and potentially harmful to humans or the environment and catalyst contamination in the synthetic products must be carefully avoided. In pursuit of nanoparticle separation, centrifugation methods have shown their inherent limitations. Long centrifugation times (on the order of hours to days) are required to achieve good separation, and even then trace nanoparticle impurities are measurable.[165] Centrifugation can also reduce nanoparticle's colloidal stability and limit the ability to reuse them in subsequent reactions.[199,200] Developing efficient alternatives to centrifugation is needed for efficient use of nanoparticle-based photocatalysts. One alternative could be acoustic separation, which uses acoustic waves to propagate through a liquid and separate particles through the generated periodic forces.[201,202] Acoustic separation may take place in flow and does not require physical contact of the nanoparticles to specialized equipment. A potent alternative that can mitigate the requirement of post-synthetic separation altogether is the adaptation of photoactive nanoparticles to packed beds in continuous flow photoreactors.[169] However, this may result in the loss of active sites and reduce their efficiency.[203,204]

Along with energy consumption concerns for the separation of nanoparticles, the energy demands for the synthesis of nanoparticles is also a concern. Here, biological pathways are of interest because they may provide more sustainable synthetic routes.[205,206172] For example, TiO_2 nanoparticles can be synthesized using *Annona squamosa* (commonly known as the custard apple) peel extract.[205] Other nanoparticles such as Ag nanoparticles may synthesized using table sugar as a reducing agent.[207] While the synthesis and use of nanoparticles is an established field, recent environmental concerns include the effects of microplastic contamination in the environment.[208] In light of this, further investigations on the environmental impacts of nanoparticles will help determine if nanoparticles are feasible for scale up and industrial adoption as heterogeneous photocatalysts.[206]

3. Polymer/ Polymer Network Photocatalysts

Polymeric heterogeneous catalysts introduce unique benefits. Their inherent modularity provides opportunities to incorporate additional stimuli responsiveness (e.g., to heat, light, pH, etc.),[209,210] or combine multiple disparate photocatalyst scaffolds (e.g., for photon upconversion).[211] Polymer-based heterogeneous photocatalysts may take the form of linear and crosslinked polymers – both conjugated and non-conjugated.

Linear Photocatalytic Polymers

Linear photocatalytic homopolymers and copolymers can be synthesized from photocatalyst monomers. For this chemical modification of photocatalysts into their respective monomers, particular consideration is important to not negatively influence photocatalytic properties. Careful monomer design has shown photocatalytic polymers being used successfully for a range of chemical transformations, e.g., RDRP,[212] hydrogen[213] or peroxide[214] production, degradation of chemicals (e.g. tetracycline),[215] and other applications.[216,217] However, synthetic products with a strong affinity towards the polymeric photocatalyst may become entangled with the catalyst and make purification prohibitively challenging. For polymerization reactions, it is important to recognize difficulties in separating linear polymer photocatalysts from polymer products. Linear polymers are typically used as homogeneous

catalysts, and therefore are not ideal candidates for heterogeneous polymerization. Nonetheless, we wanted to include this class here as proper solvent choice may help in separating products from catalysts.

Linear Conjugated Polymers

The limited solubility of conjugated polymers in many organic solvents – in tandem with their widely tunable bad gaps – makes this class of materials interesting for heterogeneous photocatalysis. Charge transfer states in conjugated polymers may be tuned by using different electron donors or acceptors, and this can be used to modify photocatalytic performance.[218] For example, Lan et. al. studied linear conjugated polymers for photocatalytic hydrogen evolution under blue light in water.[219] Notably, the polymer conformation impacted the hydrogen evolution rate, with bent structures underperforming almost four-fold when compared to the linear structure. A 20% decline in hydrogen production was found over 3 cycles (5 hours each), but performance was regenerated with the addition of more triethanolamine. To the best of our knowledge, linear conjugated polymers have yet to be used for photo-RDRP, but they may provide an interesting and effective approach due to different solubilities between conjugated and non-conjugated polymers. However, conjugated polymer networks have demonstrated notable capabilities in heterogeneous photocatalysis (see the section below dedicated to *conjugated polymer-based photocatalysts*).

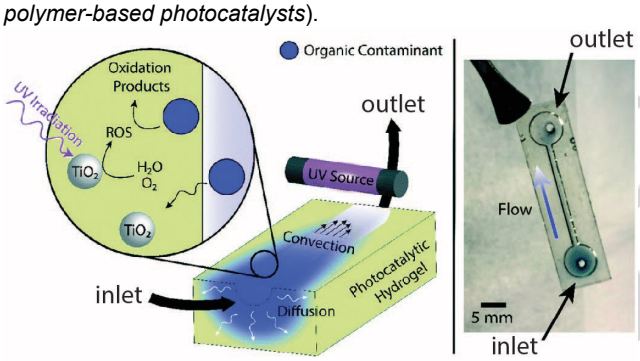

Figure 5. Photocatalytic gel reactor produced by Katzenberg et. al. featuring TiO_2 nanoparticle photocatalysts for the degradation of methylene blue. Reproduced from ref. [234] Copyright (2020) with permission from the Royal Society of Chemistry.

Pseudo-homogeneous Polymer Networks

Alternative approaches have been developed to introduce the benefits of photocatalytic monomers into heterogeneous catalysis. Many of these alternatives leverage selective or reduced solubility in the reaction medium. For example, "pseudo-homogeneous" polymeric photocatalysts contain regions which are partially soluble and can help with separation by solvent extraction.[190,220,221] A pseudo-homogeneous copolymer nanogel was produced by Ferguson and co-workers.[222] A photocatalyst monomer was copolymerized with *N*-isopropyl acrylamide and the resulting photocatalytic networks were studied for photocatalytic degradations, oxidation of styrene, and the formation of disulfide bridges. Notably, the temperature responsiveness of these catalysts allows for recovery and reuse upon heating, i.e., phase separation of the nanogels from the solvents.

Polymer Networks

Crosslinked photocatalyst-functionalized polymer networks (or polymer gels) may be composed of either fully organic or hybrid materials that contain TiO_2 or other nanoparticles.[223] The dimensions of photocatalytic gels are highly customizable and can be on the order of mm to cm to facilitate recovery through physical means after the reaction (e.g., removal by tweezers). Other examples have also shown gels on the nanoscale.[224–226] Further, solvent penetration (or the degree of network swelling) can be modified by varying the degree of crosslinking.[227] As such, depending on their design, gels may enhance reaction kinetics through diffusion into the gel resulting favorable microenvironments and increase active catalytic area.[228–231] Photocatalytic polymer gels have been studied for hydrogen production,[228] wastewater treatment,[225,232] dye degradation,[216] and RDRP.[224,233]

Because their macroscopic shapes and sizes are highly customizable,[227] polymer networks provide promising opportunities for continuous flow applications. For example, gels can either be used for packed beds,[232] or as photoreactors which afford flow of reactants through channels within the photoactive gel itself.[234] This approach was leveraged by Katzenberg et. al.,[234] who demonstrated a continuous flow reactor fabricated from a hydrogel composed ~1 wt% TiO_2 nanoparticle photocatalysts encased in a copolymer of hydroxyethyl methacrylate and acrylic acid, which was crosslinked by ethylene glycol and dimethoxy-2-phenylacetophenone (as crosslinker and photoinitiator, respectively, (see **Figure 5**). Photodegradation of methylene blue was carried out in the channels of ~1 mm diameter and ~26 mm length, reaching ~20% removal at a flow rate of 5 mL/h under UV light. While leaching substrates into the gel reduced performance, further work could reduce substrate diffusion into the gel and increase degradation by e.g., modifying crosslinking densities or choosing network materials that are less soluble with the reagents.

Multi-responsive Photocatalytic Polymer Networks

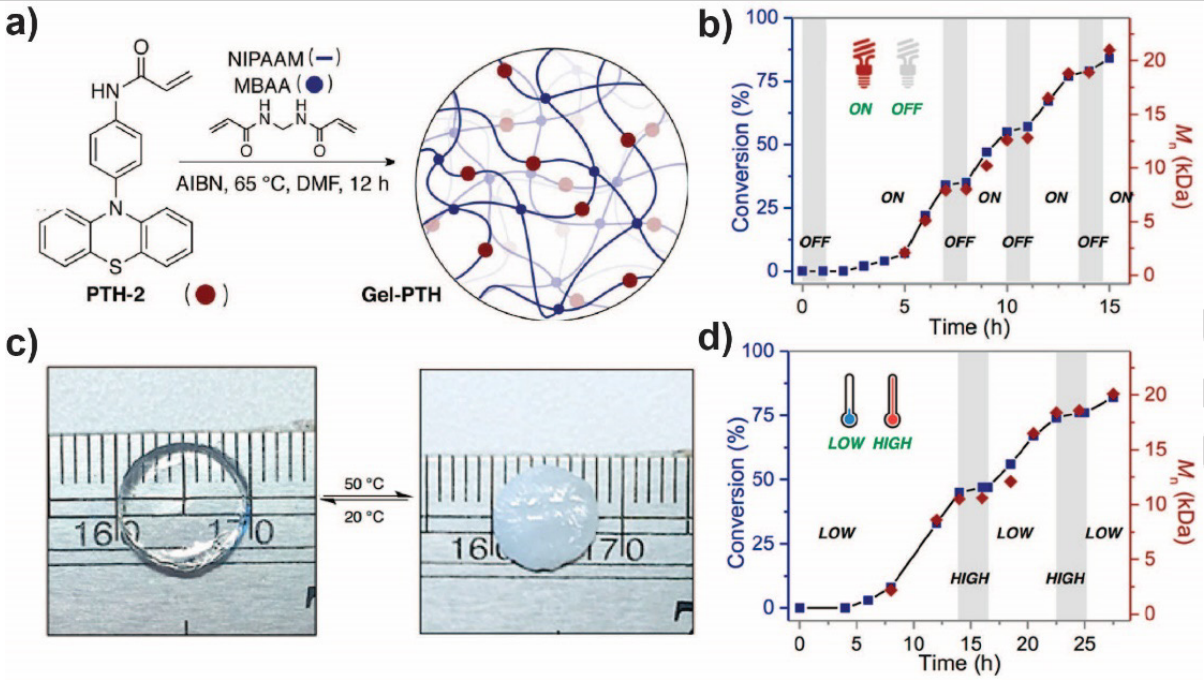

Figure 6. a) Schematic of chemical synthesis of phenyl-phenothiazine-based gel catalyst (gel-PTH), containing *N*,*N*-methylenebis(acrylamide) and *N*-isopropylacrylamide comonomers. b) Kinetics of temporal polymerization of *N*-isopropylacrylamide, featuring on/off switching of polymerization with light. c) Photographs illustration the lower critical solution temperature (LCST) behaviour of the gel-PTH photocatalyst. d) Temperature-controlled polymerization of *N*-isopropylacrylamide using gel-PTH photocatalyst. Reproduced from ref. [224] Copyright (2017), with permission from American Chemical Society.

An additional benefit of photocatalyst gels is the ability to introduce dual responsiveness. Chen et. al. synthesized a polymer gel network by crosslinking 10-phenylphenothiazine (PTH) photocatalyst-monomer and *N*-isopropylacrylamide with *N*,*N*-methylenebis(acrylamide) (see **Figure 6 & Table 1**).[224] The resulting thermoresponsive photocatalytic gel was used for the polymerization of various monomers, including vinyl acetate, acrylates, and acrylamides to conversions exceeding 90% in 10 hours, with molecular weights ranging from 14,800 to 46,600 g/mol. Low dispersity ($Đ$ < 1.2) and good retention of catalytic ability were found for at least 6 uses. Notably, the photocatalytic gel's ability to respond to heat as a second stimulus can be leveraged to activate or deactivate the gel. When subjected to heat, the gel shrinks and is reversibly deactivated, such that polymerization can be turned on or off (see **Figure 6c**). Heat treatment renders the gel collapsed and opaque, with the solvent no longer able to penetrate the polymer network. This collapsed state deactivates polymerization. It is unclear, however, whether the now opaque gel prevents catalyst activity through steric hindrance (mass transfer limitations of regents to catalytic sites) or limited light penetration. This work highlights the importance of compatibility between the photocatalytic gels and the reaction solvent. Swelling ratios studied via the weights of the gels were performed. Less swelling in acetonitrile ($W_{swollen}/W_{dry} \approx 3$) enabled more recycles without significantly sacrificing performance when compared to the better solvent, dimethyl formamide ($W_{swollen}/W_{dry} \approx 6$). More suitable solvents resulted in more efficient swelling of the networks, which can reduce their structural integrity and can limit recyclability as the gels may weaken under stress.[224,235]

Interpenetrating Polymer Networks

A potential means to improve gel lifetime in good solvents is the inclusion of a second, more robust, polymer network. The resulting materials are interpenetrating networks comprised of two or more disparate crosslinked polymers that are held together through physical interactions.[236] Li et. al. leveraged this approach and synthesized interpenetrating network gels that incorporated Eosin Y photocatalytic motifs (~2.4 mol% Eosin Y across both networks).[233] The gels showed good control over dispersity ($Đ$ <1.2) for molecular weights on the order of $M_n \approx 20{,}000$ g/mol and only a 12% decline was found in conversion over 6 reuse cycles for PET-RAFT polymerization of dimethyl acrylamide. Notably, control studies with the single network Eosin Y polymer gel exhibited a decline in conversion of approximately 40% over the same 6 reuse cycles. The single network gel color visibly faded over the reaction cycles, suggesting that the use of interpenetrating networks can indeed improve photocatalyst stability (see **Figure 7 & Table 1**). The authors suggest the decrease in recyclability observed for the single network gel may arise from the potential blockage of catalytic sites by polymers during the polymerization, or by a deactivation or loss of Eosin Y catalysts on the surface of the gel.

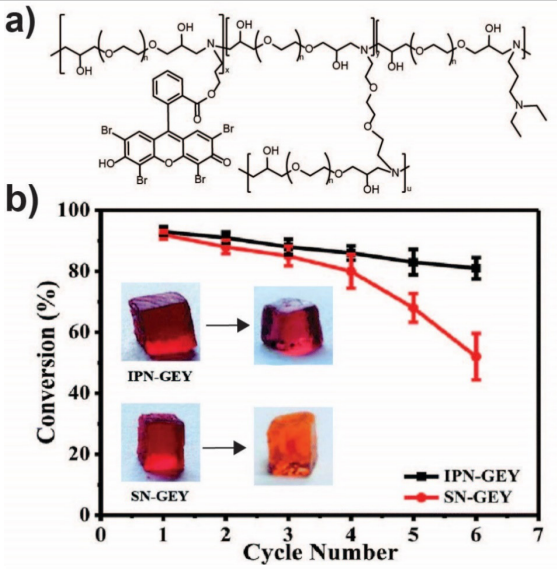

Figure 7. a) Chemical structure of polymer network containing Eosin Y photocatalytic groups (SN-GEY). b) Recyclability of interpenetrating network Eosin Y-based photocatalytic gel (IPN-GEY) versus single network (SN-GEY) counterpart for the PET-RAFT polymerization of dimethylacrylamide. Reproduced from ref. [233] Copyright (2020), with permission from the Royal Society of Chemistry.

Conjugated Polymer-Based Photocatalysts

Conjugated polymer networks tend to not swell regardless of solvent choice because of their strong π-conjugation and tightly crosslinked structures – yet they may disperse more readily depending on the polarity of the solvent.[237] Such high conjugation may be achieved by integrating the photocatalyst into the scaffold as a homo- or copolymer.[238] Extended conjugation increases the potential for catalysis via sunlight, as Xiao et. al. showed, a conjugated porous polymer comprised of ethidium bromide and triformylbenzene was effective for the reversible complexation-

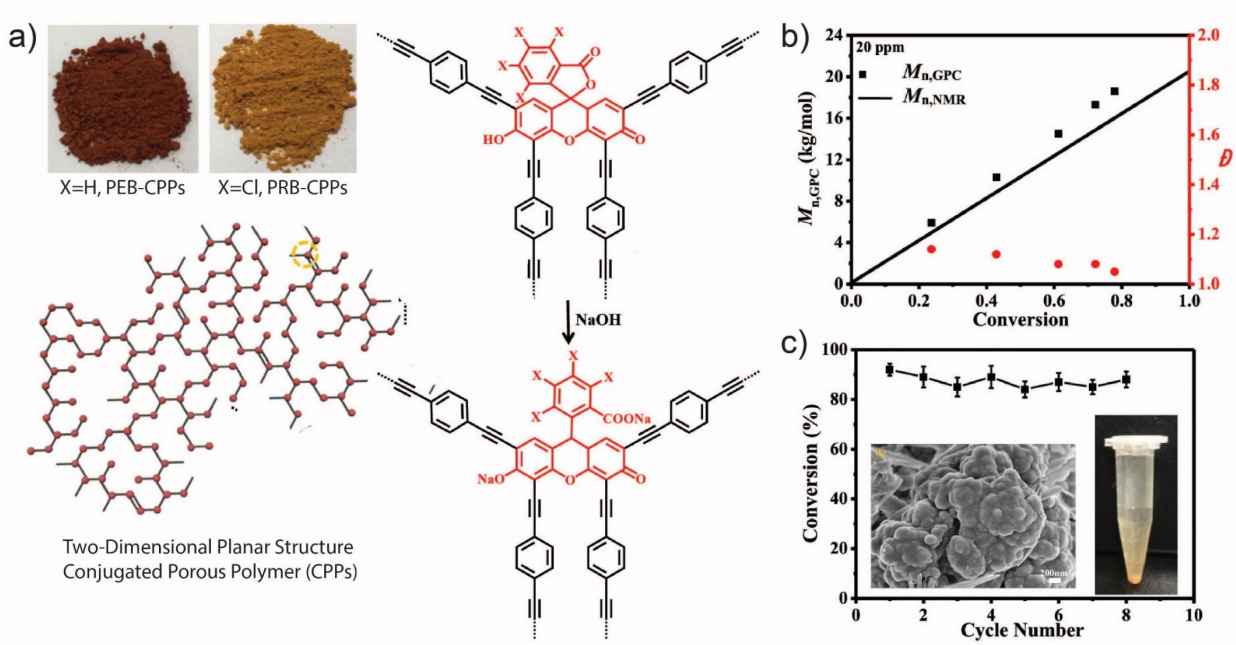

Figure 8. a) Chemical structure, appearance, and schematic of polymer erythrosine B conjugated porous polymer (PEB)-CPP and polymer rose Bengal porous polymer (PRB)-CPP. B) Kinetics of dimethylacrylamide polymerization with PEB-CPP photocatalyst under green LED irradiation. c) Average conversion of dimethyl acrylamide after 12 h with recycling, and field-emission scanning electron microscopy image of PEB-CPP, scale bar is 200 nm. Reproduced from ref. [245] Copyright (2020), with permission from American Chemical Society.

mediated radical polymerization (RCMP, $Đ$ < 1.4) of MMA under sunlight without stirring.[239]

Conjugated polymer networks – referred to in literature also as conjugated porous polymers (CPPs) or covalent organic frameworks (COFs), provide tunable pore sizes.[240] CPPs are different from COFs in that COFs provide crystalline structures while CPPs provide amorphous materials.[241] In addition CPPs provide π-conjugation, while COFs may feature π conjugation, but not necessarily. [237,242] CPPs and COFs have proven useful in a variety of photocatalytic syntheses such as PET-RAFT polymerization,[27] aza-Henry reactions,[243] and hydrogen generation.[244]

CPPs are classified by pore sizes, such as mesoporous (2-50 nm) or microporous (>50 nm).[242] Smaller pore sizes are specially classified as conjugated microporous polymers (CMPs), which feature pore sizes < 2 nm.[237] CMPs are a popular photocatalyst material, with the small pore sizes affording special features that warrant differentiation from CPPs in general. CMPs and their applications, as well as their outlook compared to COFs are expertly detailed in a review by Lee et. al.[237]

Examples suggest that conjugated systems may enhance PC longevity. Li et. al. synthesized a 2-dimensional fully conjugated polymer based on erythrosine B and Rose Bengal lactone, conjugated with 1,2-diethynylbenzene (see **Figure 8 & Table 1**).[245] This approach was theorized to improve the interactions between PC and RAFT chain transfer agent through confinement in structures while also increasing the photocatalyst stability through π-conjugation. This increased conjugation also resulted in a broadening of the absorption ranges compared to homogeneous erythrosine B and Rose Bengal, extending, and enhancing absorption from the homogenous 450-580 nm range to 250-750 nm in the conjugated systems. The resulting materials were used for the PET-RAFT polymerization of dimethylacrylamide with conversions exceeding 80% with molecular weights on the order of M_n ≈

20,000 g/mol for a total of 8 cycles after recovery through centrifugation. This suggests high catalyst stability as each polymerization cycle was performed for 12 hours. Therefore, the developed photocatalysts demonstrated 96 hours of performance without appreciable decline in efficiency. The authors also state that the catalyst may be rejuvenated with Soxhlet extraction, suggesting that blockage of pores decreases performance, but this can be remediated, and catalyst decomposition is insignificant. Hence, this work provides evidence that conjugated networks may extend PC lifetimes in comparison to homogeneous or non-conjugated approaches.

CMPs used as cocatalysts also appear to result in seemingly long-lasting PCs. For example, Dadashi-Silab et. al. synthesized a PTZ catalyst-based CMP network conjugated with dimethoxybenzene (PTZ-CMP, see **Figure 9 & Table 1**) for copper-catalyzed ATRP.[246] Conjugation results in longer wavelengths for photocatalyst activation – allowing use of UV-active PTZ (λ_{max}=300 nm in acetonitrile) under visible light irradiation, with PTZ-CMP showing absorption of wavelengths even above 600 nm. The use of milder wavelengths inherently increases catalyst stability while also reducing undesired side-product formation.[246] The micron-scale polymer networks with a 33 Å pore diameter were able to achieve high conversions and good control over ATRP with green 520 nm light ($Đ \leq 1.1$, conversion < 90%, for molecular weights ranging from M_n = 7,400 - 20,300 g/mol) of a variety of acrylate monomers under green light. No significant change was observed in conversion or dispersity over the span of 6 reaction cycles and recovery by centrifugation.

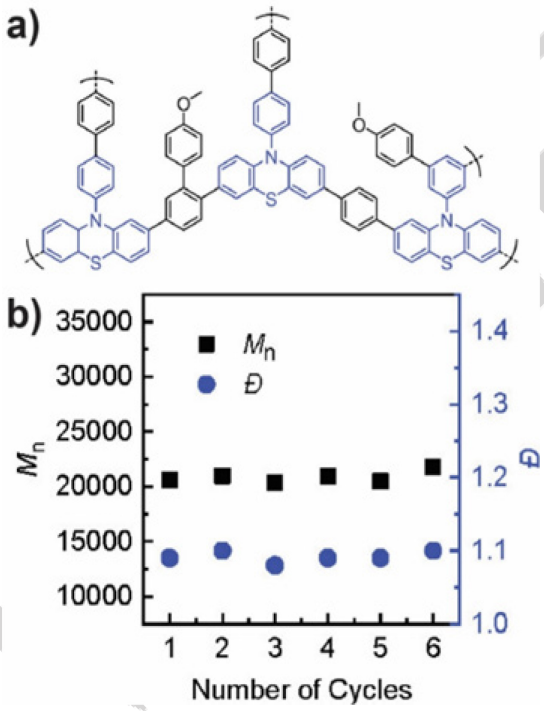

Figure 9. a) Chemical structure of 10-phenylphenothiazine-based conjugated microporous polymer (PTZ-CMP). b) Molecular weight and dispersity of methyl acrylate polymerization using PTZ-CMP over multiple cycles. Reproduced from ref. [246] Copyright (2021), with permission from American Chemical Society.

CPP pore sizes are not always reported, but some examples indicate possible pore clogging as a potential limitation. Zhao et. al. developed a porphyrinic porous polymer with imidazolium bromide moieties, referred to as TPP-ImBr-CPP, which exhibited a microporous structure and could be recovered through centrifugation.[27] Their PC demonstrated efficacy for the PET-RAFT polymerization of a variety of acrylates and methyl methacrylate, with conversions ranging from 82-93% under blue light (460 nm) in 4 hours of reaction time. Dispersity was also low ($Đ \leq 1.23$ in each case) for a range of molecular weights M_n = 18,600 - 30,400 g/mol. The TPP-ImBr-CPP catalyst could be recycled at least 5 times for the polymerization of methyl methacrylate, with a 5% decline in conversion over the recycles. Investigations determined a decrease in the catalyst BET surface area from 110 to 95 m^2/g over these recycles, indicating potential polymer product clogging the pores.

Along with pore sizes, CPP geometries also warrant consideration. CPPs may also be engineered for particular geometries, such as nanosheets, which may improve the optical properties of the catalysts, allowing for deeper penetration of light into the reaction medium as a result of higher surface area ratios achieved by 2D catalysts. Polyphthalocyanine-based conjugated network 2D structures were fabricated for the PET-RAFT polymerization of methyl acrylate by Wei et al.[247] The PCs notably demonstrated efficacy in the NIR region (760-850 nm), resulting from the conjugated system's delocalized π electrons. No apparent decline in conversion was seen across 5 cycles of polymerization and chain extensions, with conversions at ~85-93% of methyl acrylate. The dispersity remained below $Đ \leq 1.2$. The catalysts could also be used under irradiation through barriers, such as paper, chicken skin, and pig skin. The catalysts retained structural integrity across the recovery via centrifugation and reuse cycles.

It remains unclear, however, if the pore size regularity and crystallinity seen in COFs confers an advantage when compared to conjugated CMPs, which feature amorphous structures with more variation in pore sizes. COF PCs for polymerization are most frequently used as initiators for free-radical polymerization[248] or as cocatalysts for ATRP.[249] There are also a few examples of COF PCs used in PET-RAFT polymerization.[250] Yang et. al., investigated COFs synthesized from either 1,3,5-tris-(4-aminophenyl)triazine or 1,3,5-tris(4-cyanophenyl)benzene and dimethoxyterephalaldehyde to produce COF PCs for "oxygen-/water-fueled" PET-RAFT polymerization.[251]

Conjugated and non-conjugated polymeric photocatalysts may also be adapted to flow settings or scale up with reactor wall coatings,[252] and packed beds.[253] A continuous flow approach with conjugated nanotube photocatalysts for PET-RAFT polymerization has also been developed, however this system requires the centrifugation of the product for catalyst recovery and recycling.[254] Membrane reactors may improve on this approach, through using membranes that retain the catalyst in the reactor while letting the polymer products pass through. This was demonstrated by Duan et. al., who created a suspended-catalyst-based membrane reactor with suspended hollow tetra(4-ethynylphenyl)-*21H-23H*-poryphrin-based conjugated microporous polymer catalysts.[255] A cascade reactor was developed such that the catalysts were effectively retained within the reactor, while the membrane allowed for simultaneous separation of the polymer products. This system demonstrated efficacy under white and red (680 nm) light for the aqueous PET-RAFT polymerization of acrylamides. A residence time of 6 hours resulted in conversions exceeding 80% for molecular weights spanning M_n = 41,200 - 138,000 g/mol. Homopolymers and block copolymers synthesized in the membrane

reactor demonstrated purities exceeding 95%, which outperformed dialysis (which removed 83% of impurities after a total of 95 hours). Reaction medium viscosity, however, remained a significant concern, with the addition and maintenance of water levels required to avoid the clogging of the membrane. Another membrane reactor was developed by Wei et. al. for a similar PC as described in the 2D polymer network example by the same author, also showing effective synthesis and purity in the synthesis of polymeric bioconjugates.[256]

Continuous flow approaches using catalyst wall-coatings have yet to be applied for RDRP (to the best of our knowledge) but may represent a promising future opportunity. For example, Liu et. al. developed conjugated photocatalytic polymer coatings on glass coils for small molecule transformations in continuous flow.[252] Perylene diimide photocatalyst coatings were engineered by injecting and evaporating the polymer solution (see **Figure 10a**). This continuous flow reactor was evaluated for a C-H bromination reaction under 450 nm blue light, at a flow rate of 250 µL/h, with a 1-hour residence time resulting in a 68% product yield (**Figure 10b**).

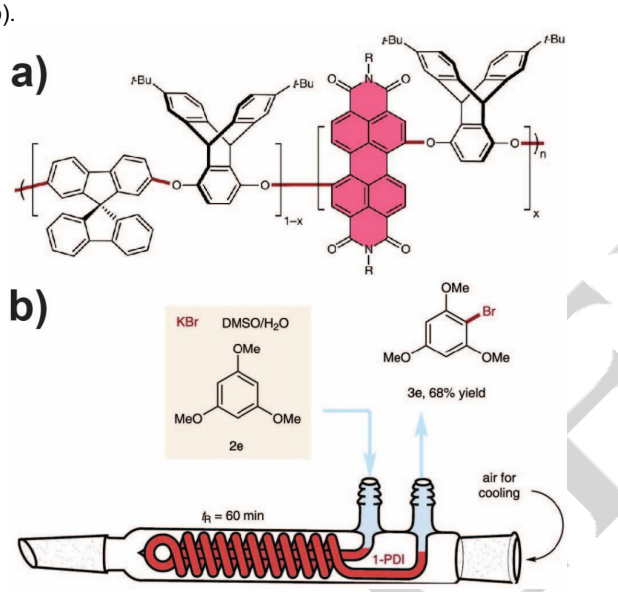

Figure 10. a) Chemical structure of perylene diimide-based conjugated photocatalyst polymer. b) Schematic of polymer-coated photocatalytic flow reactor for C-H bromination. Reproduced from ref. [252] Copyright (2022), with permission from Nature under the Creative Commons CC BY license.

Outlook for Polymer Networks

Various non-conjugated and conjugated polymer networks have shown promise in their ability to produce small and macromolecular synthetic products through photocatalysis. While gels demonstrate potential, certain limitations must be recognized and considered. Generally, compatibility between the networks and reaction solvents must be carefully chosen. Incompatible solvents reduce diffusivity of substrates through the gels, which can decrease synthetic yields, while good solvents appear to reduce the recyclability of the gel. Another consideration that may limit practicality is that gels require thorough rinsing and soaking in solvent between each reuse cycle. This could limit the use of these materials in batch settings, as synthetic products may build up within the networks and reduce access to active sites over subsequent reaction cycles. Gel dimensions are another important parameter, as penetration of light into the gel will be reduced with increasing incorporation of photocatalysts and gel size (Beer-Lambert Law). Consequently, gels may exhibit non-uniform catalytic performance with their centers showing less efficiency, therefore gel-designs that feature non-absorbing comonomers are favorable. Near IR-absorbing gels also provide fruitful opportunities going forward. However, limited work exists to date on gels that catalyze photo-RDRP resulting – in part – from some of the challenges outlined above. Additional future work on optimizing swelling and catalyst loadings could further improve recyclability and efficacy for polymer synthesis. For conjugated polymer networks, further investigations detailing pore sizes could further improve their performance in RDRP. Further investigation into continuous flow photoreactors using CPPs with careful investigation on CPP pore-clogging and subsequent active site losses could also provide interesting new prospects. Overall, polymer networks offer exciting opportunities for tunability and stimuli responsiveness while maintaining good catalytic performance.

4. Metal Organic Framework Photocatalysts

Metal organic frameworks (MOFs) are hybrid structures comprised of metals that coordinate with organic linkers.[257] As a result, MOFs can be modified by introducing photoactive sites on both the metals and ligands, or can use linkers to encapsulate the photocatalysts within the pores.[258] Using these approaches, MOFs have been functionalized with carbazoles,[259] xanthene dyes,[260] pyrene,[261] and other photocatalytic groups[258,259] and have shown efficiency for the neutralization of hazardous gases,[261] hydrogen generation,[262] as well as in organic transformations.[263,264] MOFs are inherently porous with tunable pore sizes – a key property that allows for good diffusion of substrates to the catalyst sites.[265–267] Simultaneously, plentiful opportunities arise to improve selectivity through modulation of the pore sizes.[268] Highlighting the importance of this porosity, breaking MOFs into smaller pieces to increase surface area has shown to not improve photocatalytic performance in some cases.[264] For a more detailed discussion of MOFs and their utility in polymerization, we refer to more focused review articles.[269–271]

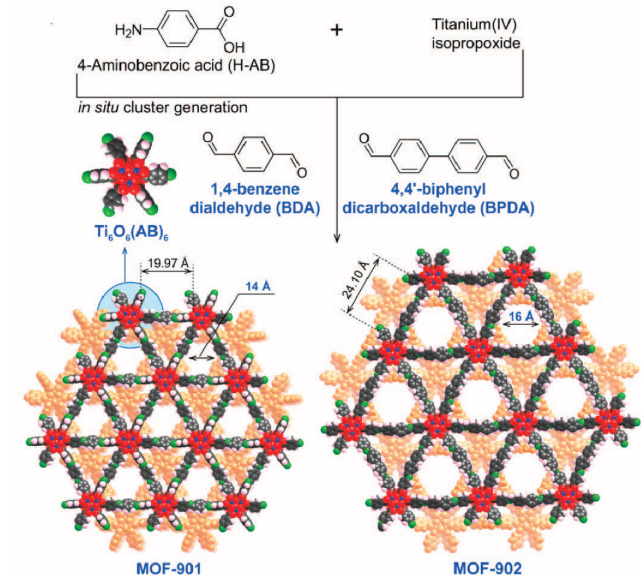

Figure 11. Structures of MOF-901 and MOF-902, used for the atom transfer radical polymerization of methyl methacrylate. Reproduced from ref. [275] Copyright (2017), with permission from American Chemical Society.

Early trials at using MOFs for polymerization showed photocatalytic free radical polymerization.[272] Nguyen et. al. synthesized a TiO_2-based MOF (MOF-901) for the ATRP of methyl methacrylate (see **Figure 11 & Table 1**).[273] An earlier example that attempted ATRP showed 87% monomer conversion was reached, but an increasing dispersity (*Đ* = 1.6) indicated a loss of control in 18 hours under compact fluorescent lighting. MOF-901 however showed no decline in performance after recovery through centrifugation over 3 reuse cycles, and notably outperformed commercial Degussa P-25 TiO_2 nanoparticles, which has been considered to have set the standard for titania photocatalysts.[274] As an alternative to MOF-901, a subsequent MOF-902 featured 4,4'-biphenyl dicarboxaldeyde (BPDA) linkers joining $Ti_6O_6(OMe)_6(AB)_6$ clusters (see **Figure 11**). [275] This extended aromatic linker (compared to MOF-901) is hypothesized to improve visible light absorption by increasing conjugation. This linker also increased the pore size of MOF-902 to 16 Å (compared to 14 Å for MOF-901). For the ATRP of methyl methacrylate, MOF-902 vastly outperformed MOF-901, reaching a conversion of 84% with a lower dispersity (*Đ* = 1.11) and molecular weights up to 31,500 g/mol. Recycling MOF-902 over 5 cycles showed only a 3% decline in conversion, with an increase in dispersity from *Đ* = 1.11 to a maximum of *Đ* = 1.20. It is unclear if the improvement in dispersity is achieved from a change in pore size, crystal structure, or the improved ability of the MOF to absorb light, but further systematic research could aid in identifying the most influential properties.

To date, there is no clear consensus on whether a given MOF design will result in polymerization within pores or predominantly on the surface of the catalyst, and the systems studied are largely for thermal polymerizations.[270] While it is possible to polymerize within MOF pores as small as ~8 Å, small pores may only accommodate a single polymer chain.[276] Such confinement effects in polymerization have been shown to decrease the reaction kinetics as a result of decreased monomer diffusion.[270,277] It is also possible that cocatalysts may not fit in the pores.[278,279] On the other hand, Mochizuki et. al. studied controlled polymerizations in MOFs and showed that nanochannels can also suppress radical termination reactions, thus narrowing the molecular weight distribution.[270] Uemura et. al. further corroborated that the molecular weight distribution of polystyrene could be decreased from *Đ* =1.7 to *Đ* = 1.5 by decreasing channel sizes from 7.5 Å to 5.7 Å.[280]

MOFs catalyzing PET-RAFT may operate on the surface of the MOF rather than inside the MOF. Zhang et. al. developed Zr-based MOFs containing Zn-metallated poryphrinic ligands, with MOF-525 (Zn) reaching 80% conversion of dimethyl acrylamide in 3 hours with *Đ* < 1.1 under yellow-green light 565 nm.[281] Interestingly, when MOF-525 (Zn) was produced at crystal sizes ranging from 0.25 to 0.77 µm, the smallest MOFs showed kinetics about 4 times faster for the polymerization of methyl acrylate, potentially resulting from the higher surface area to mass ratio seen in the smallest size (688 m^2/g compared to 327 m^2/g in the largest size). This suggests that polymerization may occur predominantly on the surface of the MOFs as opposed to within the MOF pores. Concentration optimization studies for a single size of MOF-525 showed less drastic changes with varied loadings. Dispersity for each pore size remained below *Đ* = 1.3. MOF-525 (Zn) also demonstrated efficacy for the synthesis of bioconjugates, and catalyst regeneration is possible by refluxing the catalysts in a solution containing zinc acetate. This afforded 10 or more total cycles of PET-RAFT polymerization .[282]

MOF geometries that are 2D rather than 3D may be more efficient for light-mediated RDRP if it is known that polymerization is unlikely to occur within the pores. A similar system of MOFs based on ZnTCPP in the form 2D nanosheets was developed in the same group, demonstrating remarkably fast kinetics with even 80% conversions of acrylamides and acrylates reached in under 18 minutes.[283] This nanosheet system did exhibit agglomeration at concentrations at 0.5 mg/mL, which limits the effectiveness at higher loadings. Other examples of 2D nanosheets for PET-RAFT polymerization include ZnTCPP systems in conjunction with porous coordination networks (PCN-134) showing cytocompatibility with Hek293 cells [284] and in human cell culture mediums[285] to expand the potential for PET-RAFT in biological settings. In general, nanosheets have emerged as a promising material for heterogeneous photocatalysis as a result in their improved optical properties compared to bulkier MOFs, which suffer from reduced light penetration in the reaction medium.

MOFs have also been used successfully as cocatalysts for RDRP. For example, an anthracene-functionalized zirconium-based MOF (NNU-28) showed success as a cocatalyst to reduce copper complexes under 520 nm and afford Cu-catalyzed ATRP of methacrylate monomers.[278] Low dispersity was achieved (*Đ* = 1.1–1.25), but because the copper complexes were not able to diffuse into the MOF pores, monomer conversions did not exceed ~60% over the course of 3 recycles. Molecular weights ranged from 8,000 to 18,000 g/mol in the polymer products that were controlled. Highlighting the required synergy with Cu complexes, the Zr-based MOFs did not achieve control over polymerization when used in the absence of copper complexes.[278]

Along with functioning as cocatalysts, MOF structures may also be used to encapsulate photocatalysts. For example, Xia et. al. demonstrated the utility of Zr-based (PCN-222) MOFs to house $CsPbI_3$ perovskite photocatalysts. This PC was successfully used for PET-RAFT polymerization of methyl methacrylate under sunlight (wavelengths of light ranging from 460-850 nm).[286] In addition, the PCs were able to polymerize styrene under red light up to ~85% conversion in 4 hours. Two chain extensions of poly(methyl methacrylate) resulted in an ultrahigh molecular weight product of 1,730,000 g/mol and *Đ* = 1.02. While investigation determined aqueous environments provide for strong confinement of the perovskites within the Zr-MOF, the use of lead-based materials represents a major potential hazard to human health and the environment.[287] This highlights the discrepancy between catalytic performance and ecological concerns, requiring appropriate risk-assessment and safety regulations to prevent human and environmental exposures.

Some reports of polymers[266] or surfactants[288] clogging MOF pores highlight that extra consideration is required for the design of MOFs for polymerization. As mentioned in the work by Zhang et. al., catalyst rejuvenation via refluxing may recover catalyst performance, suggesting that catalyst clogging may be a greater concern than MOF photodegradation.[281] Perhaps catalysis on the surface of the MOF may offer increased longevity by reducing polymer pore clogging.

Outlook for Metal Organic Framework Photocatalysts

In summary, MOFs represent a major class of heterogeneous photocatalysts that offer porous structures with large surface areas. MOFs have proven useful for RDRP, but further work is needed to determine pore sizes and linkers best suited for fast kinetics and low dispersities. Since MOFs may tailor pore sizes for single chains, they may prove useful for more fundamental applications where mechanistic insights may be gained. However, further investigation is needed to determine if polymerization occurs within the MOF, or on the MOF surface, as this may further aid and inform MOF design. Thermal systems for polymerization show evidence that dispersities may be lowered in tailored pore sizes, but evidence for MOFs catalyzing RDRP seems to suggest that these systems are photocatalytic mainly on the surface. It is unclear if pore clogging is the main cause of these observations.

5. Solid-Supported Photocatalysts

The tethering or immobilization of photocatalysts to inert solid supports provides unique benefits. In contrast to nanoparticle surface modification, *macroscopic* solid supports can facilitate catalyst recovery or provide structural scaffolding to support the catalyst within complex 3D structures. Common support materials include inorganics (e.g., glass),[289–293] organics (e.g., plastic beads),[294,295] or insoluble biomaterials (e.g., cellulose).[32,296] Generally, inexpensive and abundant support platforms also provide potential to increase sustainability in heterogeneous photocatalysis.

Inorganic Supports

Glass supports (SiO_x) are inexpensive, transparent for much of the photocatalysis-relevant optical spectrum, and can be readily modified through versatile silane chemistry, such as alkoxysilanes or chlorosilanes.[297] Modifying glass surfaces with these groups is experimentally well-established. For example, 3-aminopropyltriethoxysilane (APTES) is a common reagent to functionalize SiO_x surfaces with reactive primary amines.[297] APTES grafting density can be modified experimentally to 2.1 - 4.2 amine groups per square nanometer.[297,298] Furthermore, glass beads are commercially available in a variety of sizes and dimensions may be chosen for continuous flow applications.[293] Spherical glass beads of sufficiently large size have been demonstrated particularly useful for photocatalysis.

While glass is chemically inert, its optical properties may provide synergistic effects in photoreactors when used as a packing material. The curvature of glass beads improves light scattering, which has been shown by Zheng et. al. to increase reaction rates in continuous flow.[299] The authors found that glass beads of ~75 µm diameter increased the reaction rates for an *E*-to-*Z* isomerization of (*E*)-prop-1-en-ylbenzene, an aryl amination, a photo-mediated hydrogen atom transfer, and an allylic alkylation. For the isomerization reaction catalyzed by homogeneous $Ir(ppy)_3$ under blue LEDs, the reactor packed with glass beads reached a yield of 80% compared to the 50% achieved by the reactor without glass beads for the same 15 minutes of residence time. However, the available SiO_x surface area must be carefully considered. There exists a tradeoff between smaller beads providing larger surface areas for catalyst grafting, but smaller sizes may result in more difficult recovery (see nanoparticles). Particle size also changes applicability in continuous flow applications as a significant pressure drop may occur because of restricted flow – especially considering increasing viscosities throughout a polymerization. For a discussion on photocatalytic and continuous flow reactors, the reader is referred to a review by McCullagh et. al.[300]

The most widely investigated photocatalyst coating is titania,[301] which can be deposited on glass surfaces through spray coating[302] or chemical deposition.[303] Studies by Verbruggen et al. have shown that coating glass beads of 2 mm diameter with TiO_2 can result in higher reaction yields for the degradation of ethylene compared to pellets, with the coated glass approach using less catalyst material.[304]

Recent years have also spawned increasing interest in surface-immobilized organic and organometallic coatings – especially considering research has indicated surface-immobilization could extend the useful lifetimes of transition metal complex and organic photocatalysts.[193] Immobilization can be pursued in the form of monolayers,[305] or surface-tethered photocatalytic polymers.[306]

The solid-supported photocatalyst monolayer approach was also employed by Barbante et. al., who produced recyclable silica-bead based photocatalysts through coupling {$[Ru(bpy)_2(mbabpy)](PF_6)_2$} to commercial amine-functionalized glass beads of 40-63 µm diameter.[307] The resulting photocatalysts were used for the synthesis of phenylthiadiazolamine under blue LEDs, reaching a yield of ~50-58% for 8 use cycles and collection with vacuum filtration. For RDRP polymerizations, it is unclear if microparticles provide enough surface area for sufficient catalyst loadings, and therefore this approach is more commonly seen with nanoparticles.

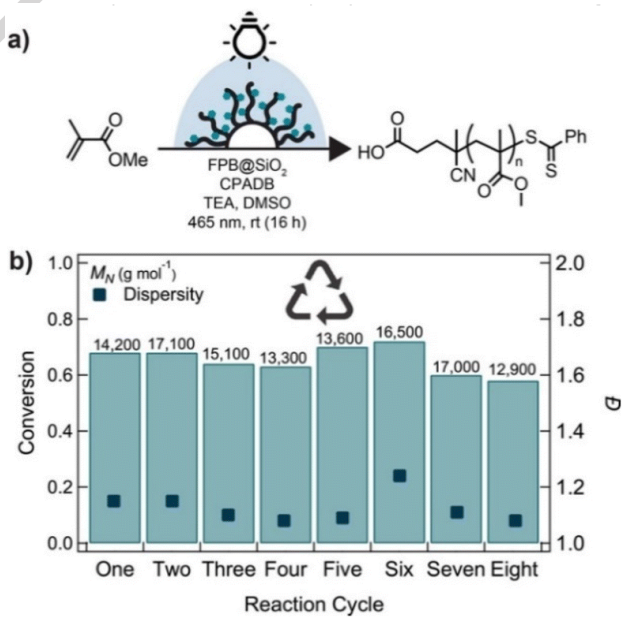

Figure 12. a) Schematic PET-RAFT polymerization of methyl methacrylate using fluorescein-based polymer brushes tethered to glass beads ($FPB@SiO_2$) in DMSO with triethyl amine (TEA) as the sacrificial electron donor, and 4-cyano-4-(phenylcarbonothioylthio)pentanoic acid (CPADB) as the RAFT agent. b) Recyclability of fluorescein-based polymer brush-coated glass beads for the PET-RAFT polymerization of methyl methacrylate. Reproduced from ref. [308] Copyright (2022), with permission from the Royal Society of Chemistry.

To increase the concentration of surface-tethered photocatalysts, photoactive polymer brushes provide promising opportunities. Bell et. al. demonstrated glass beads as useful supports for photocatalytic copolymer brushes.[306,308] Fluorescein o-acrylate was copolymerized with methyl acrylate at varying mol.% from the surface of micron-sized (< 106 µm) glass beads using a surface-initiated RAFT approach. The resulting heterogeneous fluorescein-based photocatalysts showed success for a cyclic condensation reaction as well as a radical dehalogenation reaction.[309] Both reactions featured recyclability, with the cyclic condensation reaction showing negligible decline in conversion over 10 uses.[306] In an extension of this work, the PC@SiO_x beads also showed good control over PET-RAFT polymerization of a variety of acrylates and methacrylates under blue light (465 nm), achieving molecular weights ranging from M_n = 10,200 up to M_n = 66,700 g/mol.[308] For the case of methyl methacrylate, good control (Đ < 1.3, conversions > 60%) and high conversions (see **Figure 12 & Table 1**) were observed. The beads were recoverable through filtration and maintained ability over the 8 cycles of use and cleaning. Polymer brushes offer added ability for customization of the local catalyst environments, as well as stimuli responsiveness. Stimuli responsiveness has been shown with thermally responsive photocatalytic brushes on silica nanoparticles that have been demonstrated for the hydrolysis of p-nitrophenyl acetate.[310] On micron-scale glass beads, stimuli responsiveness to heat has also been shown with NIPAAM comonomers used with fluorescein-based photocatalytic polymer brushes to enhance photocatalytic activity upon heating.[311] In addition, polymer brush composition can be tailored to enhance the longevity of surface attachment of grafted molecules.

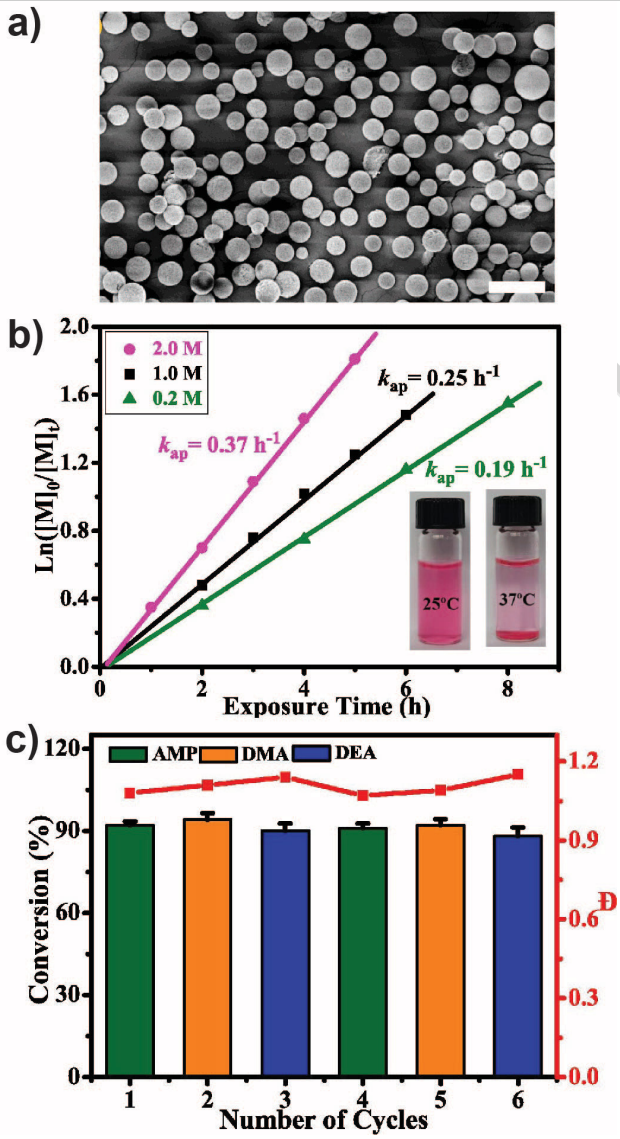

Figure 13. a) Scanning electron micrograph of the nanofibrous chitin microspheres functionalized with a N-isopropylacrylamide and Eosin Y-acrylate-based polymer (NCPNIEY; scale bar is 100 µm). b) Kinetics of 4-acryloylmorpholine polymerization at different concentrations with NCPNIEY photocatalysts. Insert shows aggregation behaviour with increased temperature, which facilitates recovery. c) Recyclability of NCPNIEY microspheres for the polymerization of 4-acryloyl morpholine, dimethyl acrylamide, and *N,N*-diethylacrylamide. Reproduced from ref. [318] Copyright (2022), with permission from Elsevier B.V

As discussed, triethoxy silanes are a common choice for covalent attachments of organics to glass, however these systems suffer from degrafting via hydrolysis.[312] To retain surface attachment, hydrophobic polymers have been demonstrated to reduce polymer brush degrafting.[313] Some potential limitations of the photocatalyst polymer brush approach are related to the "grafting from" method, which requires the synthesis and tethering of a polymerization initiator (and e.g., adds cost and effort for RAFT or ATRP initiators).[314] Moreover, during synthesis of the photocatalyst, appreciable amounts of polymer catalysts grown in solution were not initiated from the tethered RAFT agents, resulting in the waste of photocatalyst monomers.

Porous SiO_2 supports can increase the available surface area for grafted catalysts, and the pore structures can lead to enhanced mass transport. For example, Marques et. al. immobilized TiO_2 nanoparticles onto micron-scale porous silica (~47 μM diameter) scaffolds.[315] The catalysts were irradiated with a Xe lamp at 255 W to simulate sunlight and were evaluated for the photocatalytic degradation of methyl orange and paracetamol in a packed bed reactor at a flow rate of 5 mL/min. Notably, when scaled for the mass of TiO_2, this system performed similarly if not better to other reported systems of similar loadings of TiO_2. In addition, the microspheres did not exhibit degradation, nor were washing treatments required between uses.

Finally, glass wool is also an attractive support material because it can increase the available surface areas for grafting photocatalysts.[290,316,317] Teixeira et. al. demonstrated the versatility of glass wool as a support through the attachment of different photocatalysts: $Ru(bpy)_2dppa(PF_6)_2$, $Ru(phen)_2dppa(PF_6)_2$, Eosin Y, antraquinone, and Rose Bengal to aminopropyl triethoxysilane-modified glass wool.[290] Each catalyst was found to be recyclable for at least four uses in the photooxidation of dimethylanthracene. As such, glass wool would also provide an interesting platform to explore for heterogenous photocatalysts in RDRP.

Organic Support Materials

Organic solid supports for photocatalysts may be comprised of polymer gels[225] or biomaterials (e.g., chitin).[318] Guo et. al. produced microsphere photocatalysts using nanofibrous chitin bead supports for Eosin Y and *N*-isopropylacrylamide copolymers (see **Figure 13 & Table 1**).[318] The obtained microspheres were evaluated for the polymerization of 4-acryloyl morpholine, dimethylacrylamide, diethylacrylamide, and other water-soluble monomers. For 4-acryloyl morpholine, the catalysts achieved notable conversions ranging from 81-99% with low dispersity (*Đ* = 1.08-1.25) for molecular weights ranging from 27,900 to ~90,000 g/mol under 520 nm irradiation. Heating to 37 °C induced aggregation as a result of the altered solubility of the material and facilitated catalyst recovery. This allowed for the photocatalysts to be reused over 6 recycles with negligible changes in conversion and dispersity.

Fibrous organic supports again provide larger surface areas to immobilize photocatalysts. Examples include polymer (PDMS) sponges[319] or cellulose in the form of cotton threads[32,296,320] – all of which can be easily removed by physical means such as tweezers. As a result of their flexibility and thin diameters, such fibrous supports can be packed into reactors of various shapes, and provide a means to scale up photocatalysis in continuous flow approaches.[319]

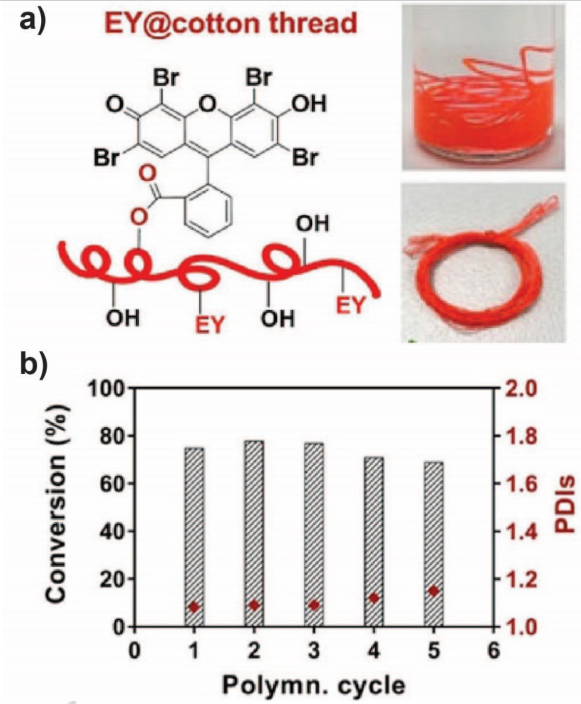

Figure 14. a) Schematic of Eosin Y-functionalized cotton threads. b) Recyclability (monomer conversion and dispersity over 6 cycles) of EY@cotton thread catalysts for the polymerization of methyl acrylate after 20 hours under green light. Reproduced from ref. [296] Copyright (2020), with permission from Wiley-VCH.

Chu et. al. synthesized a carboxylic acid-functionalized variant of zinc tetraphenylporyphrin (ZnTPP) that could be reacted with hydroxyl groups on cellulose supports.[32] The resulting ZnTPP@cellulose photocatalysts were effective for the PET-RAFT polymerization of acrylates and methacrylates under 635 nm light. For example, 72% methyl methacrylate conversion was observed in 24 hours (*Đ* = 1.08), and molecular weights ranged from 6,000 to 27,100 g/mol. The cotton scaffold fared better than the cellulose sponge, likely due to better light penetration through the fibers as opposed to the porous system. However, both demonstrated significant loss in efficacy: the cotton scaffold dropped from 65% to 36% conversion over the course of 5 cycles, whereas the cellulose sponge scaffold dropped from ~59% to 28% over the same 5 recycles. Conversion declines were likely a result of demetallation of the Zn centers, with ~30% of the original loading of Zn lost from the complexes per use.

To mitigate this metal leaching, fully organic photocatalyst alternatives have also been studied tethered to cotton threads for PET-RAFT. Chu et. al. immobilized Eosin Y onto cotton threads (EY@cotton, see **Figure 14 & Table 1**) and demonstrated improved recyclability compared to ZnTPP@cellulose system.[296] Five recycles were performed for the polymerization of methyl acrylate. A decline in conversion was seen from 75% on the first cycle to 69% on the 5th cycle (**Figure 14b**). Less than 0.3 μg of Eosin Y was leached into the solution with each cycle, indicating only minor catalyst contamination in the final product.

Tetraphenylporphyrin-functionalized cotton thread supports were also successfully used in continuous flow for PET-RAFT polymerization.[88] Dimethylacrylamide conversion of 65% was reached with a 10 hour residence time with a flow rate of 1.93 μL/min. Notably, the system maintained conversions (within 2%) for 20 hours. In batch settings, the catalyst demonstrated recyclability for at

least 5 cycles. Both batch and flow achieved molecular weights of about 15,000 g/mol, indicating no apparent mixing or viscosity concerns at this targeted molecular weight. This study represents one of the few current examples of a heterogeneous photocatalytic RDRP in continuous flow. In comparison, for homogeneous photocatalytic systems, RDRP can achieve molecular weights that range from ~3500 g/mol (*Đ* = 1.5, flow rate = 1 μL/min)[321] to up to 106,000 g/mol (*Đ* = 1.22, flow

rate = 30 μL /min).[322] Viscosities and flow regimes, such as turbulent or laminar, are major factors affecting the polymer products, with the potential for different molecular weights at different depths within the reactor.[323] Heterogeneous systems are expected to add potential challenges related to inhomogeneities within the reactor, increased pressure drops across the flow regions, and decreased light penetration. Consequently, it is uncertain to date what limitations on molecular weights will be found for these new systems.

Outlook for Solid-Supported Photocatalysts

Using solid supports – fibrous materials (e.g., cotton or cellulose) or glass beads – can present desirable means for the heterogenization of photocatalysts. Support materials must be carefully considered for chemical compatibility as well as for their capacity to provide adequate catalyst loadings. Limitations for fibrous supports include potential irregularities of packing density in chemical reactors, possibly resulting in non-uniform reaction rates throughout the medium. Fibrous supports in batch settings may also reduce the efficient mixing of reactants. It can also be challenging to fine tune the amount of tethered photocatalysts. Grafting densities are pre-determined through the available functional groups on the supports and the efficiency of both the chosen functionalization chemistry and possible steric hindrance play significant roles. Notably, this contrasts with polymer networks, where catalyst incorporation (and characterization thereof) is facilitated. Further work in this arena could further develop the feasibility of RDRP in continuous flow settings.

Table 1: Summary of Heterogeneous PCs for RDRP
Details provided in the table are for the recycled catalysts conditions if available

Catalyst	RDRP Type(s)	Monomer	Solvent	Light Source λ_{max}	Mn, *Đ*	Number of Cycles	Ref(s)
Nanoparticles							
ZnO[a]	ATRP	MMA	MeCN	350 nm	8,100, *1.23*	N/A	176
Fe-doped ZnO[a]	ATRP	MMA	MeCN	350 nm	11,900, *1.18*	N/A	176
Eosin Y@SiO_2	PET-RAFT	*n*-BA	NMP	515 nm	~10,000, *1.13-1.16*	5	166
β-$NaYF_4$,Yb^{3+}, Tm^{3+} @SiO_2[a]	ATRP	MA	DMSO	980 nm	~16,000, ~*1.25*	5	15
$UCNP^+$@SiO_2@N-CDs[a]	ATRP	MMA	DMF	980 nm	N/A	5	197
Mercaptopropionic acid-capped CdSe QDs	PET-RAFT	DMA	Water	532 nm	6000-14,300, *1.03-1.20*	5	165
$CsPbBr_3$ nanocrystals	PET-RAFT	MA,BA,TFEA	Toluene	480 nm	2,200-40,000, *≤1.09*	N/A	182
Polymer Networks/Gels							
Gel-PTH	PET-RAFT[b],ATRP[b], photoiniferter	NIPAAM	MeCN	14 W CFL	~21,000, *<1.20*	6	224
PTZ-CMP[a]	ATRP	MA	MeCN	520 nm	~21,000, *≤1.1*	6	246
Eosin Y IPN Gel	PET-RAFT	DMA	Water	520 nm	N/A	6	233
PEB-CPP	PET-RAFT	DMA	DMSO	520 nm	N/A	8	245
TPP-ImBr-CPP	PET-RAFT	MMA	DMSO	460 nm	~16,000[c], *1.2*[c]	5	27
PPc-n; PPc-p	PET-RAFT	MA	DMSO	760 nm; 850 nm	~8500-42,500[d], *<1.2;* ~9,500-47,500[d],*<1.2*	5 (w/ chain extensions)	247
TAPPy-TPA-COF[a]	ATRP	MMA	MeCN	White LED	12,600-5,400,*1.14-1.22*	4	249
TAPT-COF	PET-RAFT	$PEGMA_{475}$	Water	White LED	N/A,*<1.5*	5	251
DMTA-COF	PET-RAFT	$PEGMA_{475}$	Water	White LED	N/A,*<1.25*	5	251
MOFs							
MOF-901	ATRP	MMA	DMF	55 W, CFL	24,900-26,900, *1.6*	3	273
MOF-902	ATRP	BMA	1,4-Dioxane	55 W, CFL	30,000-32,000, *1.11-1.20*	5	275
MOF-525 (Zn)	PET-RAFT	MA	DMSO	565 nm	14,800-18500,*≤1.18*	6	281
NNU-28[a]	ATRP	MMA	MeCN	520 nm Xe arc lamp	N/A	3	278
$CsPbI_3$@PCN-222	PET-RAFT	MMA	DMSO	850 nm	~17,000, *<1.15*	6	286
Solid-supported PCs							
Fluorescein-based polymer brush@SiO_2 beads	PET-RAFT	MMA	DMSO	465 nm	12,900-17,100,*<1.3*	8	308
Eosin Y-based polymers@chitin microspheres	PET-RAFT	AMP,DMA,DEA	Water	520 nm	N/A,<1.2	6	318
ZnTPP@cotton	PET-RAFT	MA	DMSO	635 nm	N/A	3	32
Eosin Y@cotton threads	PET-RAFT	MA	DMSO	530 nm	N/A, *≤1.20*	5	296
TPP-TA-N@cotton threads	PET-RAFT	DMA	DMSO	530 nm	N/A,<1.15	5	88

[a] Cocatalyst. [b] Not shown for recycling experiments. [c] Results for final cycle. [d] Chain-extension. N/A denotes not available. Monomer abbreviations are as follows: MA: methyl acrylate; MMA: methyl methacrylate; *n*-BA: *n*-Butyl acrylate; DMA: dimethylacrylamide; NIPAAM: N-Isopropylacrylamide;BMA: Benzyl methacrylate; TFEA: 2,2,2-Trifluoroethyl acrylate,$PEGMA_{475}$: Poly(ethylene glycol) methacrylate, DEA: *N,N*-Diethyacrylamide, AMP: 4-Acryloylmorpholine

6. Summary and Outlook

Heterogeneous photocatalytic systems combine the benefits of sustainable photocatalysis with simplified purification procedures. As outlined throughout this article, research on heterogeneous photocatalysis has shown great promise for catalytic performance and recyclability, often demonstrating efficacy after many cycles of use. Herein, we discussed four categories: (i) nanoparticles, (ii) polymer networks, (iii) metal-organic frameworks (MOFs), and (iv) solid supported PCs , **Table 1** highlights selected literature examples and their performance in recycling. We discussed examples, advantages, and limitations of photocatalytic nanoparticles, polymer networks, metal-organic frameworks, and solid supported photocatalysts on various porous and non-porous substrates. In

brief, nanoparticles have demonstrated efficacy, but material losses in recovery by centrifugation still represent a significant limitation. Polymer networks have also shown promise, but challenges arise from polymer swelling and dispersion. MOFs have been studied for controlled polymerization, but further investigation is needed to determine how pore sizes affect efficacy and reusability. Finally, solid supports offer readily available materials, but mass transfer limitations due to their macroscopic sizes must be considered.

Generally, increased understanding and further improvements are required to leverage the full benefits of these (and other) heterogeneous photocatalysis on larger scales. A more detailed elaboration on light intensities and irradiation timeframes would benefit future researchers to compare new systems to established approaches. Material stability also requires further investigation as it is not yet completely understood how to select PCs for long-term use. To this end, a more comprehensive understanding of photobleaching of immobilized photocatalysts would benefit the field significantly.

Many reports of heterogeneous photocatalysts document catalyst choice as the result of only a few trials with only a few of the commercially available xanthene dyes with single-step modifications. More thorough analyses of catalyst behavior in their relevant environments could lead to enhanced designs that are able to balance desired catalyst activity with the desired catalyst stability. Particularly for heterogeneous photo-RDRP, a focus in literature has been on PET-RAFT polymerizations and expansion towards photo-ATRP could provide interesting findings.

Scaling up photocatalysts as continuous processes and for industrial adoption still presents significant challenges. For continuous flow applications, an ideal scenario would involve catalysts with high stability and durability to assure active functionality without catalyst rejuvenation or replacement of the packed bed. As heterogeneous photocatalysts are developed, recycling studies that extend the duration until significant decline is observed would aid further understanding of catalyst lifetimes. Many heterogeneous photocatalysis studies in continuous flow to date operate on flow rates ranging on the order of microliters to milliliters per minute. Scaling-up of such lab-scale reactors is non-trivial as material selection, light penetration, and pressure regulation all become considerable obstacles. Increased viscosities in polymer-containing reaction mediums are also expected to result in significant challenges with respect to operating pressures and heterogeneous packed photoreactors are expected to further exacerbate this challenge.

In conclusion, heterogeneous photocatalysis offers great potential in providing for a sustainable future. However, given the success of the organic photocatalysts detailed in this review, it is feasible that even more effective non-TiO_2-based catalysis may be discovered and established for these applications. As such, the future holds great promise for these materials to realize more sustainable and effective means to control both the construction and deconstruction of polymers.

Acknowledgements

The authors acknowledge the NSF CBET Award # 2143628 for financial support.

Keywords: Heterogeneous catalysis • Photocatalysis • Polymers • Surface chemistry • Sustainable chemistry

References

[1] J. Scaiano, *Light Photochemistry*, American Chemical Society, Washington, DC, USA, **2022**.
[2] Q.Y. Lee, H. Li, *Micromachines*., **2021**, *12*,.
[3] Z. Ouyang, Y. Yang, C. Zhang, S. Zhu, L. Qin, W. Wang, D. He, Y. Zhou, H. Luo, F. Qin, *J. Mater. Chem. A*., **2021**, *9*, 13402–13441.
[4] N. Corrigan, M. Ciftci, K. Jung, C. Boyer, *Angew. Chemie Int. Ed.*, **2021**, *60*, 1748–1781.
[5] P. Lu, D. Ahn, R. Yunis, L. Delafresnaye, N. Corrigan, C. Boyer, C. Barner-Kowollik, Z.A. Page, *Matter*., **2021**, *4*, 2172–2229.
[6] I. Ghosh, B. König, *Angew. Chemie Int. Ed.*, **2016**, *55*, 7676–7679.
[7] S. Shanmugam, J. Xu, C. Boyer, *Macromol. Rapid Commun.*, **2017**, *38*, 1700143.
[8] S. Aubert, M. Bezagu, A.C. Spivey, S. Arseniyadis, *Nat. Rev. Chem.*, **2019**, *3*, 706–722.
[9] M.H. Shaw, J. Twilton, D.W.C. MacMillan, *J. Org. Chem.*, **2016**, *81*, 6898–6926.
[10] M. Fromel, M. Li, C.W. Pester, *Macromol. Rapid Commun.*, **2020**, *41*, 2000177.
[11] G. Panzarasa, G. Soliveri, *Appl. Sci.*, **2019**, *9*, 1266.
[12] J.M. Herrmann, *Environ. Sci. Pollut. Res.*, **2012**, *19*, 3655–3665.
[13] B. Li, Y. Hu, Z. Shen, Z. Ji, L. Yao, S. Zhang, Y. Zou, D. Tang, Y. Qing, S. Wang, G. Zhao, X. Wang, *ACS ES&T Eng.*, **2021**, *1*, 947–964.
[14] P. Bharmoria, H. Bildirir, K. Moth-Poulsen, *Chem. Soc. Rev.*, **2020**, *49*, 6529–6554.
[15] W. Zhang, J. He, C. Lv, Q. Wang, X. Pang, K. Matyjaszewski, X. Pan, *Macromolecules*., **2020**, *53*, 4678–4684.
[16] N.A. Romero, D.A. Nicewicz, *Chem. Rev.*, **2016**, *116*, 10075–10166.
[17] S. Reischauer, B. Pieber, *IScience*., **2021**, *24*, 102209.
[18] A. Alvarez-Martin, S. Trashin, M. Cuykx, A. Covaci, K. De Wael, K. Janssens, *Dye. Pigment.*, **2017**, *145*, 376–384.
[19] R.H. Crabtree, *Chem. Rev.*, **2012**, *112*, 1536–1554.
[20] J.A. Widegren, R.G. Finke, *J. Mol. Catal. A Chem.*, **2003**, *198*, 317–341.
[21] A. Savateev, M. Antonietti, *ACS Catal.*, **2018**, *8*, 9790–9808.
[22] H.L. Tan, F.F. Abdi, Y.H. Ng, *Chem. Soc. Rev.*, **2019**, *48*, 1255–1271.
[23] S. Gisbertz, B. Pieber, *ChemPhotoChem.*, **2020**, *4*, 456–475.
[24] M.A. Fox, M.T. Dulay, *Chem. Rev.*, **1993**, *93*, 341–357.
[25] Q. Wang, T. Hisatomi, Q. Jia, H. Tokudome, M. Zhong, C. Wang, Z. Pan, T. Takata, M. Nakabayashi, N. Shibata, Y. Li, I.D. Sharp, A. Kudo, T. Yamada, K. Domen, *Nat. Mater.*, **2016**, *15*, 611–615.
[26] Z. Xie, C. Wang, K.E. Dekrafft, W. Lin, *J. Am. Chem. Soc.*, **2011**, *133*, 2056–2059.
[27] M. Zhao, S. Zhu, X. Yang, Y. Wang, X. Zhou, X. Xie, *Macromol. Rapid Commun.*, **2022**, *43*, 2200173.
[28] P. Rana, R. Gaur, B. Kaushik, S. Yadav, P. Yadav, P. Sharma, M.B. Gawande, R.K. Sharma, *J. Catal.*, **2021**, *401*, 297–308.
[29] X. Li, S. Ye, Y.C. Zhang, H.P. Zhao, Y. Huang, B. Zhang, T. Cai, *Nanoscale*., **2020**, *12*, 7595–7603.
[30] Á. Molnár, A. Papp, *Coord. Chem. Rev.*, **2017**, *349*, 1–65.

[31] K. Teegardin, J.I. Day, J. Chan, J. Weaver, *Org. Process Res. Dev.*, **2016**, *20*, 1156–1163.
[32] Y. Chu, Z. Huang, K. Liang, J. Guo, C. Boyer, J. Xu, *Polym. Chem.*, **2018**, *9*, 1666–1673.
[33] S. Mosleh, M.R. Rahimi, M. Ghaedi, K. Dashtian, S. Hajati, *RSC Adv.*, **2016**, *6*, 63667–63680.
[34] C.Y. Toe, J. Pan, J. Scott, R. Amal, *ACS ES T Eng.*, **2022**, *2*, 1130–1143.
[35] C.G. Thomson, A.L. Lee, F. Vilela, *Beilstein J. Org. Chem.*, **2020**, *16*, 1495–1549.
[36] J.Z. Bloh, R. Marschall, *European J. Org. Chem.*, **2017**, *2017*, 2085–2094.
[37] S. Gisbertz, B. Pieber, *ChemPhotoChem.*, **2020**, *4*, 456–475.
[38] A.O. Ibhadon, P. Fitzpatrick, *Catal. 2013, Vol. 3, Pages 189-218.*, **2013**, *3*, 189–218.
[39] H. Wang, X. Li, X. Zhao, C. Li, X. Song, P. Zhang, P. Huo, *Chinese J. Catal.*, **2022**, *43*, 178–214.
[40] A. Bagheri, C.M. Fellows, C. Boyer, *Adv. Sci.*, **2021**, *8*, 2003701.
[41] M. Li, M. Fromel, D. Ranaweera, S. Rocha, C. Boyer, C.W. Pester, *ACS Macro Lett.*, **2019**, *8*, 374–380.
[42] L.H. Rong, X. Cheng, J. Ge, O.K. Krebs, J.R. Capadona, E.B. Caldona, R.C. Advincula, *ACS Appl. Polym. Mater.*, **2022**, *4*, 6449–6457.
[43] D. Gong, W.C.J. Ho, Y. Tang, Q. Tay, Y. Lai, J.G. Highfield, Z. Chen, *J. Solid State Chem.*, **2012**, *189*, 117–122.
[44] B. Li, B. Yu, Q. Ye, F. Zhou, *Acc. Chem. Res.*, **2015**, *48*, 229–237.
[45] J.D. Jeyaprakash, S. Samuel, R. Dhamodharan, J. Rühe, *Macromol. Rapid Commun.*, **2002**, *23*, 277–281.
[46] J. Pyun, T. Kowalewski, K. Matyjaszewski, *Macromol. Rapid Commun.*, **2003**, *24*, 1043–1059.
[47] T. Chen, I. Amin, R. Jordan, *Chem. Soc. Rev.*, **2012**, *41*, 3280–3296.
[48] A.M. Wong, D.J. Valles, C. Carbonell, C.L. Chambers, A.Y. Rozenfeld, R.W. Aldasooky, A.B. Braunschweig, *ACS Macro Lett.*, **2019**, *8*, 1474–1478.
[49] S. Dadashi-Silab, C. Aydogan, Y. Yagci, *Polym. Chem.*, **2015**, *6*, 6595–6615.
[50] H.J. Hageman, *Prog. Org. Coatings.*, **1985**, *13*, 123–150.
[51] K. Parkatzidis, H.S. Wang, N.P. Truong, A. Anastasaki, *Chem.*, **2020**, *6*, 1575–1588.
[52] C. Fu, J. Xu, M. Kokotovic, C. Boyer, *ACS Macro Lett.*, **2016**, *5*, 444–449.
[53] A.J. Gormley, J. Yeow, G. Ng, Ó. Conway, C. Boyer, R. Chapman, *Angew. Chemie Int. Ed.*, **2018**, *57*, 1557–1562.
[54] S. Shanmugam, J. Cuthbert, T. Kowalewski, C. Boyer, K. Matyjaszewski, *Macromolecules.*, **2018**, *51*, 7776–7784.
[55] R. Barbey, L. Lavanant, D. Paripovic, N. Schüwer, C. Sugnaux, S. Tugulu, H.A. Klok, *Chem. Rev.*, **2009**, *109*, 5437–5527.
[56] W. Yan, S. Dadashi-Silab, K. Matyjaszewski, N.D. Spencer, E.M. Benetti, *Macromolecules.*, **2020**, *19*, 34.
[57] S. Xu, J. Yeow, C. Boyer, *ACS Macro Lett.*, **2018**, *7*, 1376–1382.
[58] A. Shahrokhinia, P. Biswas, J.F. Reuther, *J. Polym. Sci.*, **2021**, *59*, 1748–1786.
[59] K. Zhang, M. Xiao, L. Zhang, Y. Chen, J. Tan, *ACS Macro Lett.*, **2022**, *11*, 716–722.
[60] V. Kottisch, Q. Michaudel, B.P. Fors, *J. Am. Chem. Soc.*, **2016**, *138*, 15535–15538.
[61] X. Zhang, Y. Jiang, Q. Ma, S. Hu, S. Liao, *J. Am. Chem. Soc.*, **2021**, *143*, 6357–6362.
[62] K.A. Ogawa, A.E. Goetz, A.J. Boydston, *J. Am. Chem. Soc.*, **2015**, *137*, 1400–1403.
[63] A.E. Goetz, L.M.M. Pascual, D.G. Dunford, K.A. Ogawa, D.B. Knorr, A.J. Boydston, *ACS Macro Lett.*, **2016**, *5*, 579–582.
[64] W. Wang, Z. Zhou, D. Sathe, X. Tang, S. Moran, J. Jin, F. Haeffner, J. Wang, J. Niu, *Angew. Chemie Int. Ed.*, **2022**, *61*, e202113302.
[65] Q. Feng, L. Yang, Y. Zhong, D. Guo, G. Liu, L. Xie, W. Huang, R. Tong, *Nat. Commun.*, **2018**, *9*, 1–10.
[66] T. Celiker, K. Kaya, S. Koyuncu, Y. Yagci, *Macromolecules.*, **2020**, *53*, 5787–5794.
[67] F. Jasinski, A. Rannée, J. Schweitzer, D. Fischer, E. Lobry, C. Croutxé-Barghorn, M. Schmutz, D. Le Nouen, A. Criqui, A. Chemtob, *Macromolecules.*, **2016**, *49*, 1143–1153.
[68] B.D. Fairbanks, T.F. Scott, C.J. Kloxin, K.S. Anseth, C.N. Bowman, *Macromolecules.*, **2009**, *42*, 211–217.
[69] N.B. Cramer, J.P. Scott, C.N. Bowman, *Macromolecules.*, **2002**, *35*, 5361–5365.
[70] N. Corrigan, K. Jung, G. Moad, C.J. Hawker, K. Matyjaszewski, C. Boyer, *Prog. Polym. Sci.*, **2020**, *111*, 101311.
[71] M. Chen, M. Zhong, J.A. Johnson, *Chem. Rev.*, **2016**, *116*, 10167–10211.
[72] K. Matyjaszewski, *Macromolecules.*, **2012**, *45*, 4015–4039.
[73] G. Szczepaniak, L. Fu, H. Jafari, K. Kapil, K. Matyjaszewski, *Acc. Chem. Res.*, **2021**, *54*, 1779–1790.
[74] D.A. Corbin, G.M. Miyake, *Chem. Rev.*, **2022**, *122*, 1830–1874.
[75] R.R. Shah, D. Merreceyes, M. Husemann, I. Rees, N.L. Abbott, C.J. Hawker, J.L. Hedrick, *Macromolecules.*, **2000**, *33*, 597–605.
[76] J. Phommalysack-Lovan, Y. Chu, C. Boyer, J. Xu, *Chem. Commun.*, **2018**, *54*, 6591–6606.
[77] Y. Lee, C. Boyer, M.S. Kwon, **2023**,.
[78] H.R. Lamontagne, B.H. Lessard, *ACS Appl. Polym. Mater.*, **2020**, *2*, 5327–5344.
[79] M.K. Brinks, A. Studer, *Macromol. Rapid Commun.*, **2009**, *30*, 1043–1057.
[80] S.B. Rahane, S.M. Kilbey, A.T. Metters, **2005**,.
[81] M. Hartlieb, *Macromol. Rapid Commun.*, **2022**, *43*, 2100514.
[82] J.D. Bell, J.A. Murphy, *Chem. Soc. Rev.*, **2021**, *50*, 9540–9685.
[83] D.M. Arias-Rotondo, J.K. McCusker, *Chem. Soc. Rev.*, **2016**, *45*, 5803–5820.
[84] C. Wu, N. Corrigan, C.H. Lim, K. Jung, J. Zhu, G. Miyake, J. Xu, C. Boyer, *Macromolecules.*, **2019**, *52*, 236–248.
[85] C. Michelin, N. Hoffmann, *ACS Catal.*, **2018**, *8*, 12046–12055.
[86] F. Lorandi, M. Fantin, K. Matyjaszewski, *J. Am. Chem. Soc.*, **2022**, *144*, 15413–15430.
[87] C. Wu, N. Corrigan, C.H. Lim, W. Liu, G. Miyake, C. Boyer, *Chem. Rev.*, **2022**, *122*, 5476–5518.
[88] Y. Chu, N. Corrigan, C. Wu, C. Boyer, J. Xu, *ACS Sustain. Chem. Eng.*, **2018**, *6*, 15245–15253.
[89] V. Bellotti, R. Simonutti, *Polymers (Basel).*, **2021**, *13*, 1119.
[90] M.L. Allegrezza, D. Konkolewicz, *ACS Macro Lett.*, **2021**, *10*, 433–446.
[91] N. Corrigan, J. Xu, C. Boyer, X. Allonas, *ChemPhotoChem.*, **2019**, *3*, 1193–1199.
[92] L.R. Kuhn, M.L. Allegrezza, N.J. Dougher, D. Konkolewicz, *J. Polym. Sci.*, **2020**, *58*, 139–144.
[93] D.M. Arias-Rotondo, J.K. McCusker, *Chem. Soc. Rev.*, **2016**, *45*, 5803–5820.

[94] R. Bevernaegie, S.A.M. Wehlin, B. Elias, L. Troian-Gautier, *ChemPhotoChem*., **2021**, *5*, 217–234.
[95] F. Dumur, *Eur. Polym. J.*, **2022**, *165*, 110999.
[96] J.R. Ochola, M.O. Wolf, *Org. Biomol. Chem.*, **2016**, *14*, 9088–9092.
[97] Y. Tong, Y. Liu, Q. Chen, Y. Mo, Y. Ma, *Macromolecules*., **2021**, *54*, 6117–6126.
[98] Z. Yang, Z. Mao, Z. Xie, Y. Zhang, S. Liu, J. Zhao, J. Xu, Z. Chi, M.P. Aldred, *Chem. Soc. Rev.*, **2017**, *46*, 915–1016.
[99] Y. Zhao, Y. Chen, H. Zhou, Y. Zhou, K. Chen, Y. Gu, M. Chen, *Nat. Synth. 2023*., **2023**, 1–10.
[100] X. Pan, C. Fang, M. Fantin, N. Malhotra, W.Y. So, L.A. Peteanu, A.A. Isse, A. Gennaro, P. Liu, K. Matyjaszewski, *J. Am. Chem. Soc.*, **2016**, *138*, 2411–2425.
[101] J. Xu, K. Jung, C. Boyer, *Macromolecules*., **2014**, *47*, 4217–4229.
[102] B.P. Fors, C.J. Hawker, *Angew. Chemie Int. Ed.*, **2012**, *51*, 8850–8853.
[103] J. Xu, K. Jung, A. Atme, S. Shanmugam, C. Boyer, *J. Am. Chem. Soc.*, **2014**, *136*, 5508–5519.
[104] N.C.M. Magdaong, M. Taniguchi, J.R. Diers, D.M. Niedzwiedzki, C. Kirmaier, J.S. Lindsey, D.F. Bocian, D. Holten, *J. Phys. Chem. A.*, **2020**, *124*, 7776–7794.
[105] J.C. Bawden, P.S. Francis, S. DiLuzio, D.J. Hayne, E.H. Doeven, J. Truong, R. Alexander, L.C. Henderson, D.E. Gómez, M. Massi, B.I. Armstrong, F.A. Draper, S. Bernhard, T.U. Connell, *J. Am. Chem. Soc.*, **2022**, *144*, 11189–11202.
[106] L. Schmid, C. Kerzig, A. Prescimone, O.S. Wenger, *J. Am. Chem. Soc.*, **2021**, *1*, 819–832.
[107] H.G. Roth, H.G. Roth, N.A. Romero, D.A. Nicewicz, **2015**,.
[108] C.K. Prier, D.A. Rankic, D.W.C. MacMillan, *Chem. Rev.*, **2013**, *113*, 5322–5363.
[109] S. Hübner, J.G. de Vries, V. Farina, *Adv. Synth. Catal.*, **2016**, *358*, 3–25.
[110] M.V. Bobo, J.J. Kuchta, A.K. Vannucci, *Org. Biomol. Chem.*, **2021**, *19*, 4816–4834.
[111] S. Sharma, A. Sharma, *Org. Biomol. Chem.*, **2019**, *17*, 4384–4405.
[112] Z. Li, H. Song, R. Guo, M. Zuo, C. Hou, S. Sun, X. He, Z. Sun, W. Chu, *Green Chem.*, **2019**, *21*, 3602–3605.
[113] D.A. Rogers, R.G. Brown, Z.C. Brandeburg, E.Y. Ko, M.D. Hopkins, G. Leblanc, A.A. Lamar, *ACS Omega*., **2018**, *3*, 12868–12877.
[114] G. Szczepaniak, J. Jeong, K. Kapil, S. Dadashi-Silab, S.S. Yerneni, P. Ratajczyk, S. Lathwal, D.J. Schild, S.R. Das, K. Matyjaszewski, *Chem. Sci.*, **2022**, *13*, 11540–11550.
[115] D.P. Haria, B. König, *Chem. Commun.*, **2014**, *50*, 6688–6699.
[116] C. Wu, N. Corrigan, C.H. Lim, K. Jung, J. Zhu, G. Miyake, J. Xu, C. Boyer, *Macromolecules*., **2019**, *52*, 236–248.
[117] J. Xu, S. Shanmugam, H.T. Duong, C. Boyer, *Polym. Chem.*, **2015**, *6*, 5615–5624.
[118] B. Nomeir, O. Fabre, K. Ferji, *Macromolecules*., **2019**, *52*, 6898–6903.
[119] D. Bondarev, K. Borská, M. Šoral, D. Moravčíková, J. Mosnáček, *Polymer (Guildf)*., **2019**, *161*, 122–127.
[120] S. Marder, S.R. Gwaltney, C.N. Scott, I. Rajapaksha, H. Chang, Y. Xiong, *J. Org. Chem.*, **2020**, *85*, 12108–12116.
[121] R. Karthik, M. Govindasamy, S.M. Chen, Y.H. Cheng, P. Muthukrishnan, S. Padmavathy, A. Elangovan, *J. Photochem. Photobiol. B Biol.*, **2017**, *170*, 164–172.
[122] B.G. McCarthy, R.M. Pearson, C.H. Lim, S.M. Sartor, N.H. Damrauer, G.M. Miyake, *J. Am. Chem. Soc.*, **2018**, *140*, 5088–5101.
[123] E.H. Discekici, N.J. Treat, S.O. Poelma, K.M. Mattson, Z.M. Hudson, Y. Luo, C.J. Hawker, J.R. De Alaniz, *Chem. Commun.*, **2015**, *51*, 11705–11708.
[124] Q. Quan, M. Ma, Z. Wang, Y. Gu, M. Chen, *Angew. Chemie Int. Ed.*, **2021**, *60*, 20443–20451.
[125] J. Zhou, L. Mao, M.X. Wu, Z. Peng, Y. Yang, M. Zhou, X.L. Zhao, X. Shi, H.B. Yang, *Chem. Sci.*, **2022**, *13*, 5252.
[126] J.C. Theriot, C.H. Lim, H. Yang, M.D. Ryan, C.B. Musgrave, G.M. Miyake, *Science (80-.)*., **2016**, *352*, 1082–1086.
[127] S.O. Poelma, G.L. Burnett, E.H. Discekici, K.M. Mattson, N.J. Treat, Y. Luo, Z.M. Hudson, S.L. Shankel, P.G. Clark, J.W. Kramer, C.J. Hawker, J. Read De Alaniz, *J. Org. Chem.*, **2016**, *81*, 7155–7160.
[128] N.J. Treat, H. Sprafke, J.W. Kramer, P.G. Clark, B.E. Barton, J. Read De Alaniz, B.P. Fors, C.J. Hawker, *J. Am. Chem. Soc.*, **2014**, *136*, 16096–16101.
[129] V.K. Singh, C. Yu, S. Badgujar, Y. Kim, Y. Kwon, D. Kim, J. Lee, T. Akhter, G. Thangavel, L.S. Park, J. Lee, P.C. Nandajan, R. Wannemacher, B. Milián-Medina, L. Lüer, K.S. Kim, J. Gierschner, M.S. Kwon, *Nat. Catal.*, **2018**, *1*, 794–804.
[130] E.P. Fonseca Parra, B. Chouchene, J.L. Six, R. Schneider, K. Ferji, *ACS Appl. Polym. Mater.*, **2021**, *3*, 3649–3658.
[131] T. Banerjee, F. Podjaski, J. Kröger, B.P. Biswal, B. V. Lotsch, *Nat. Rev. Mater.*, **2020**, *6*, 168–190.
[132] V. Bellotti, K. Parkatzidis, H.S. Wang, N. De Alwis Watuthanthrige, M. Orfano, A. Monguzzi, N.P. Truong, R. Simonutti, A. Anastasaki, *Polym. Chem.*, **2022**, *14*, 253–258.
[133] R. Cao, M.Q. Zhang, C. Hu, D. Xiao, M. Wang, D. Ma, *Nat. Commun.*, **2022**, *13*, 1–10.
[134] A. Beltrán, M. Mikhailov, M.N. Sokolov, V. Pérez-Laguna, A. Rezusta, M.J. Revillo, F. Galindo, *J. Mater. Chem. B.*, **2016**, *4*, 5975–5979.
[135] A.P. Demchenko, *Methods Appl. Fluoresc.*, **2020**, *8*, 022001.
[136] J.K.G. Karlsson, O.J. Woodford, R. Al-Aqar, A. Harriman, *J. Phys. Chem. A.*, **2017**, *121*, 8569–8576.
[137] H. Kisch, D. Bahnemann, *J. Phys. Chem. Lett.*, **2015**, *6*, 1907–1910.
[138] J.J. Devery, J.J. Douglas, J.D. Nguyen, K.P. Cole, R.A. Flowers, C.R.J. Stephenson, *Chem. Sci.*, **2015**, *6*, 537–541.
[139] N.T. Vo, Y. Mekmouche, T. Tron, R. Guillot, F. Banse, Z. Halime, M. Sircoglou, W. Leibl, A. Aukauloo, *Angew. Chemie Int. Ed.*, **2019**, *58*, 16023–16027.
[140] K. Matyjaszewski, S. Coca, S.G. Gaynor, M. Wei, B.E. Woodworth, *Macromolecules*., **1998**, *31*, 5967–5969.
[141] J. Yeow, R. Chapman, A.J. Gormley, C. Boyer, *Chem. Soc. Rev.*, **2018**, *47*, 4357–4387.
[142] G. Ng, J. Yeow, J. Xu, C. Boyer, *Polym. Chem.*, **2017**, *8*, 2841–2851.
[143] S. Xu, G. Ng, J. Xu, R.P. Kuchel, J. Yeow, C. Boyer, *ACS Macro Lett.*, **2017**, *6*, 1237–1244.
[144] N. Corrigan, D. Rosli, J.W.J. Jones, J. Xu, C. Boyer, *Macromolecules*., **2016**, *49*, 6779–6789.
[145] A.E. Enciso, L. Fu, A.J. Russell, K. Matyjaszewski, *Angew. Chemie Int. Ed.*, **2018**, *57*, 933–936.
[146] S.E. Seo, E.H. Discekici, Y. Zhang, C.M. Bates, C.J. Hawker, *J. Polym. Sci.*, **2020**, *58*, 70–76.
[147] L. Zhang, C. Wu, K. Jung, Y.H. Ng, C. Boyer, *Angew. Chemie Int. Ed.*, **2019**, *58*, 16811–16814.
[148] S. Peiris, J. McMurtrie, H.-Y. Zhu, *Catal. Sci. Technol.*, **2016**, *6*,

320–338.
[149] J. Kosco, M. Bidwell, H. Cha, T. Martin, C.T. Howells, M. Sachs, D.H. Anjum, S. Gonzalez Lopez, L. Zou, A. Wadsworth, W. Zhang, L. Zhang, J. Tellam, R. Sougrat, F. Laquai, D.M. DeLongchamp, J.R. Durrant, I. McCulloch, *Nat. Mater.*, **2020**, *19*, 559–565.
[150] K. Mondal, A. Sharma, *RSC Adv.*, **2016**, *6*, 83589–83612.
[151] P. V Kamat, *J. Phys. Chem. B.*, **2002**, *106*, 7729–7744.
[152] A. Fujishima, T.N. Rao, D.A. Tryk, *J. Photochem. Photobiol. C Photochem. Rev.*, **2000**, *1*, 1–21.
[153] A. FUJISHIMA, K. HONDA, *Nature.*, **1972**, *238*, 37–38.
[154] D.L. Liao, B.Q. Liao, *J. Photochem. Photobiol. A Chem.*, **2007**, *187*, 363–369.
[155] F. Han, V.S.R. Kambala, M. Srinivasan, D. Rajarathnam, R. Naidu, *Appl. Catal. A Gen.*, **2009**, *359*, 25–40.
[156] G. Liu, X. Li, J. Zhao, H. Hidaka, N. Serpone, *Environ. Sci. Technol.*, **2000**, *34*, 3982–3990.
[157] R. Verma, S. Singh, M.K. Dalai, M. Saravanan, V. V. Agrawal, A.K. Srivastava, *Mater. Des.*, **2017**, *133*, 10–18.
[158] X. Zhao, Z. Li, Y. Chen, L. Shi, Y. Zhu, *Appl. Surf. Sci.*, **2008**, *254*, 1825–1829.
[159] J. Schneider, M. Matsuoka, M. Takeuchi, J. Zhang, Y. Horiuchi, M. Anpo, D.W. Bahnemann, *Chem. Rev.*, **2014**, *114*, 9919–9986.
[160] Q. Guo, C. Zhou, Z. Ma, X. Yang, *Adv. Mater.*, **2019**, *31*, 1901997.
[161] Q. Xiao, J. Zhang, C. Xiao, Z. Si, X. Tan, *Sol. Energy.*, **2008**, *82*, 706–713.
[162] I. Barton, V. Matejec, J. Matousek, *J. Photochem. Photobiol. A Chem.*, **2016**, *317*, 72–80.
[163] W. Chairungsri, A. Subkomkaew, P. Kijjanapanich, Y. Chimupala, *Chemosphere.*, **2022**, *286*, 131762.
[164] N.P. Radhika, R. Selvin, R. Kakkar, A. Umar, *Arab. J. Chem.*, **2019**, *12*, 4550–4578.
[165] K.P. McClelland, T.D. Clemons, S.I. Stupp, E.A. Weiss, *ACS Macro Lett.*, **2020**, *9*, 7–13.
[166] S. Shanmugam, S. Xu, N.N.M. Adnan, C. Boyer, *Macromolecules.*, **2018**, *51*, 779–790.
[167] Y. Zhu, E. Egap, *ACS Polym. Au.*, **2021**, *1*, 76–99.
[168] S. Linic, P. Christopher, D.B. Ingram, *Nat. Mater.*, **2011**, *10*, 911–921.
[169] J. Farah, F. Malloggi, F. Miserque, J. Kim, E. Gravel, E. Doris, *Nanomaterials.*, **2023**, *13*, 1184.
[170] C.B. Ong, L.Y. Ng, A.W. Mohammad, *Renew. Sustain. Energy Rev.*, **2018**, *81*, 536–551.
[171] M. Hara, T. Kondo, M. Komoda, S. Ikeda, J. N. Kondo, K. Domen, M. Hara, K. Shinohara, A. Tanaka, *Chem. Commun.*, **1998**, 357–358.
[172] K. Dulta, G. Koşarsoy Ağçeli, P. Chauhan, R. Jasrotia, P.K. Chauhan, J.O. Ighalo, *Sustain. Environ. Res.*, **2022**, *32*, 2.
[173] L. Cheng, Q. Xiang, Y. Liao, H. Zhang, *Energy Environ. Sci.*, **2018**, *11*, 1362–1391.
[174] W. Ho, J.C. Yu, *J. Mol. Catal. A Chem.*, **2006**, *247*, 268–274.
[175] X. Qiao, Q. Wang, G. shi, Y. He, X. Pang, *Polym. Chem.*, **2022**, *13*, 5873–5881.
[176] S. Dadashi-Silab, M. Atilla Tasdelen, A. Mohamed Asiri, S. Bahadar Khan, Y. Yagci, *Macromol. Rapid Commun.*, **2014**, *35*, 454–459.
[177] S. Peiris, J. McMurtrie, H.Y. Zhu, *Catal. Sci. Technol.*, **2016**, *6*, 320–338.
[178] S. Lv, Y. Du, F. Wu, Y. Cai, T. Zhou, *Nanoscale Adv.*, **2022**, *4*, 2608–2631.
[179] S. Linic, P. Christopher, D.B. Ingram, *Nat. Mater.*, **2011**, *10*, 911–921.
[180] X. Zhang, X. Ke, H. Zhu, *Chem. – A Eur. J.*, **2012**, *18*, 8048–8056.
[181] C.B. Ong, L.Y. Ng, A.W. Mohammad, *Renew. Sustain. Energy Rev.*, **2018**, *81*, 536–551.
[182] Y. Zhu, Y. Liu, K.A. Miller, H. Zhu, E. Egap, *ACS Macro Lett.*, **2020**, *9*, 725–730.
[183] D.Y.C. Leung, X. Fu, C. Wang, M. Ni, M.K.H. Leung, X. Wang, X. Fu, *ChemSusChem.*, **2010**, *3*, 681–694.
[184] M. Khan, M.E. Assal, M.N. Tahir, M. Khan, M. Ashraf, M.R. Hatshan, M. Khan, R. Varala, N.M. Badawi, S.F. Adil, *J. Saudi Chem. Soc.*, **2022**, *26*, 101544.
[185] Y. Shemesh, J.E. Macdonald, G. Menagen, U. Banin, *Angew. Chemie.*, **2011**, *123*, 1217–1221.
[186] J. Rubio-Cervilla, E. González, J.A. Pomposo, *Nanomaterials.*, **2017**, *7*,.
[187] S. Sarina, H. Zhu, E. Jaatinen, Q. Xiao, H. Liu, J. Jia, C. Chen, J. Zhao, *J. Am. Chem. Soc.*, **2013**, *135*, 5793–5801.
[188] M.J.R. Virlan, D. Miricescu, R. Radulescu, C.M. Sabliov, A. Totan, B. Calenic, M. Greabu, *Molecules.*, **2016**, *21*,.
[189] W. Qingyao, C. Jingjing, W. Xiao, L. Yan, Z. Yajie, H. Wang, Y. Liu, W. Hui, L. Fan, S. Mingwang, K. Zhenghui, *Nat. Commun.*, **2021**, *12*, 483.
[190] S. Kim, K. Landfester, C.T.J. Ferguson, *ACS Nano.*, **2022**, *16*, 17041–17048.
[191] R.B. Nasir Baig, R.S. Varma, *ACS Sustain. Chem. Eng.*, **2013**, *1*, 805–809.
[192] S. Shanmugam, S. Xu, N.N.M. Adnan, C. Boyer, *Macromolecules.*, **2018**, *51*, 779–790.
[193] J.C.S. Terra, A. Desgranges, Z. Amara, A. Moores, *Catal. Today.*, **2023**, *407*, 52–58.
[194] T.N. Singh-Rachford, F.N. Castellano, *Coord. Chem. Rev.*, **2010**, *254*, 2560–2573.
[195] B.S. Richards, D. Hudry, D. Busko, A. Turshatov, I.A. Howard, *Chem. Rev.*, **2021**, *121*, 9165–9195.
[196] C. Ding, J. Wang, W. Zhang, X. Pan, Z. Zhang, W. Zhang, J. Zhu, X. Zhu, *Polym. Chem.*, **2016**, *7*, 7370–7374.
[197] X. Qiao, Q. Hao, M. Chen, G. Shi, Y. He, X. Pang, *ACS Appl. Mater. Interfaces.*, **2022**, *14*, 21555–21563.
[198] Manoswini, D. Bhattacharya, P. Sen, N. Ganguly, P.S. Mohanty, *Adv. Nat. Sci. Nanosci. Nanotechnol.*, **2021**, *12*, 25003.
[199] J. Midelet, A.H. El-Sagheer, T. Brown, A.G. Kanaras, M.H. V. Werts, *Part. Part. Syst. Charact.*, **2017**, *34*, 1700095.
[200] Z. Hussain, S. Sahudin, **2016**.
[201] M. Wu, Z. Mao, K. Chen, H. Bachman, Y. Chen, J. Rufo, L. Ren, P. Li, L. Wang, T.J. Huang, *Adv. Funct. Mater.*, **2017**, *27*, 1606039.
[202] M. Wu, A. Ozcelik, J. Rufo, Z. Wang, R. Fang, T. Jun Huang, *Microsystems Nanoeng.*, **2019**, *5*, 1–18.
[203] J. Silvestre-Albero, A. Sepúlveda-Escribano, F. Rodríguez-Reinoso, J.A. Anderson, *J. Catal.*, **2004**, *223*, 179–190.
[204] W. Ji, X. Wang, M. Tang, L. Yang, Z. Rui, Y. Tong, J.Y.S. Lin, *Chem. Commun.*, **2019**, *55*, 6846–6849.
[205] S.M. Roopan, A. Bharathi, A. Prabhakarn, A. Abdul Rahuman, K. Velayutham, G. Rajakumar, R.D. Padmaja, M. Lekshmi, G. Madhumitha, *Spectrochim. Acta Part A Mol. Biomol. Spectrosc.*, **2012**, *98*, 86–90.
[206] F. Wu, Z. Zhou, A.L. Hicks, *Environ. Sci. Technol.*, **2019**, *53*, 4078–4087.

[207] S. Nazir, A. Muazzam, M. Ismail, *J Biosci Tech.*, **2011**, *2*, 425–430.
[208] J.A. Ivar Do Sul, M.F. Costa, *Environ. Pollut.*, **2014**, *185*, 352–364.
[209] M. Wei, Y. Gao, X. Li, M.J. Serpe, *Polym. Chem.*, **2017**, *8*, 127–143.
[210] F.R. Wurm, C. Boyer, B.S. Sumerlin, *Macromol. Rapid Commun.*, **2021**, *42*, 2100512.
[211] M. Sittig, B. Schmidt, H. Görls, T. Bocklitz, M. Wächtler, S. Zechel, M.D. Hager, B. Dietzek, *Phys. Chem. Chem. Phys.*, **2020**, *22*, 4072–4079.
[212] J.J. Lessard, G.M. Scheutz, A.B. Korpusik, R.A. Olson, C.A. Figg, B.S. Sumerlin, *Polym. Chem.*, **2021**, *12*, 2205–2209.
[213] M. Sachs, R.S. Sprick, D. Pearce, S.A.J. Hillman, A. Monti, A.A.Y. Guilbert, N.J. Brownbill, S. Dimitrov, X. Shi, F. Blanc, M.A. Zwijnenburg, J. Nelson, J.R. Durrant, A.I. Cooper, *Nat. Commun.*, **2018**, *9*, 1–11.
[214] L. Liu, M.Y. Gao, H. Yang, X. Wang, X. Li, A.I. Cooper, *J. Am. Chem. Soc.*, **2021**, *143*, 19287–19293.
[215] T. Yang, E. Zhu, H. Guo, J. Du, Y. Wu, C. Liu, G. Che, *ACS Appl. Mater. Interfaces.*, **2021**, *13*, 51447–51458.
[216] T. Kuckhoff, K. Landfester, K.A.I. Zhang, C.T.J. Ferguson, *Chem. Mater.*, **2021**, *33*, 9131–9138.
[217] H. Koizumi, Y. Shiraishi, S. Tojo, M. Fujitsuka, T. Majima, T. Hirai, **2023**, *19*, 3.
[218] T. Marszalek, M. Li, W. Pisula, *Chem. Commun.*, **2016**, *52*, 10938–10947.
[219] Z. Lan, G. Zhang, X. Chen, Y. Zhang, K.A.I. Zhang, X. Wang, *Angew. Chemie Int. Ed.*, **2019**, *58*, 10236–10240.
[220] R. Li, J. Heuer, T. Kuckhoff, K. Landfester, C. Ferguson, *Angew. Chemie Int. Ed.*, **2023**,.
[221] M.J. Bu, C. Cai, F. Gallou, B.H. Lipshutz, *Green Chem.*, **2018**, *20*, 1233–1237.
[222] C.T.J. Ferguson, N. Huber, K. Landfester, K.A.I. Zhang, *Angew. Chemie Int. Ed.*, **2019**, *58*, 10567–10571.
[223] N.X.D. Mai, J. Bae, I.T. Kim, S.H. Park, G.W. Lee, J.H. Kim, D. Lee, H. Bin Son, Y.C. Lee, J. Hur, *Environ. Sci. Nano.*, **2017**, *4*, 955–966.
[224] M. Chen, S. Deng, Y. Gu, J. Lin, M.J. MacLeod, J.A. Johnson, *J. Am. Chem. Soc.*, **2017**, *139*, 2257–2266.
[225] Q. Cao, J. Barrio, M. Antonietti, B. Kumru, M. Shalom, B.V.K.J. Schmidt, *ACS Appl. Polym. Mater.*, **2020**, *2*, 3346–3354.
[226] J. Byun, K. Landfester, K.A.I. Zhang, *Chem. Mater.*, **2019**, *31*, 3381–3387.
[227] K. Hearon, K. Gall, T. Ware, D.J. Maitland, J.P. Bearinger, T.S. Wilson, *J. Appl. Polym. Sci.*, **2011**, *121*, 144–153.
[228] P. Verma, D. Samanta, P. Sutar, A. Kundu, J. Dasgupta, T.K. Maji, *ACS Appl. Mater. Interfaces.*, **2022**,.
[229] B. Maiti, A. Abramov, R. Pérez-Ruiz, D. Díaz Díaz, *Acc. Chem. Res.*, **2019**, *52*, 1865–1876.
[230] J. Heuer, C.T.J. Ferguson, *Nanoscale.*, **2022**, *14*, 1646–1652.
[231] A.S. Weingarten, R. V. Kazantsev, L.C. Palmer, M. McClendon, A.R. Koltonow, A.P.S. Samuel, D.J. Kiebala, M.R. Wasielewski, S.I. Stupp, *Nat. Chem.*, **2014**, *6*, 964–970.
[232] C. Dong, J. Lu, B. Qiu, B. Shen, M. Xing, J. Zhang, *Appl. Catal. B Environ.*, **2018**, *222*, 146–156.
[233] X. Li, Y.C. Zhang, S. Ye, X.R. Zhang, T. Cai, *J. Mater. Chem. A.*, **2020**, *8*, 25363–25370.
[234] A. Katzenberg, A. Raman, N.L. Schnabel, A.L. Quispe, A.I. Silverman, M.A. Modestino, *React. Chem. Eng.*, **2020**, *5*, 377–386.
[235] K.S. Anseth, C.N. Bowman, L. Brannon-Peppas, *Biomaterials.*, **1996**, *17*, 1647–1657.
[236] K. Ashida, K. Iwasaki, *THERMOSETTING FOAMS*, K. Ashida, K. IwasakiHandb. Plast. Foam., Elsevier, **1995**: pp. 11–220p. 11–220.
[237] J.S.M. Lee, A.I. Cooper, *Chem. Rev.*, **2020**, *120*, 2171–2214.
[238] J. Sun, H.S. Jena, C. Krishnaraj, K. Singh Rawat, S. Abednatanzi, J. Chakraborty, A. Laemont, W. Liu, H. Chen, Y.-Y. Liu, K. Leus, H. Vrielinck, V. Van Speybroeck, P. van der Voort, *Angew. Chemie Int. Ed.*, **2023**,.
[239] L. Xiao, Q. Li, Y. Liu, X. Fu, Y. Zhao, J. Cai, X. Yin, L. Hou, *Polym. Chem.*, **2021**, *12*, 6714–6723.
[240] J. Guo, D. Jiang, *ACS Cent. Sci.*, **2020**, *6*, 869–879.
[241] S.-Y. Ding, W. Wang, *Chem. Soc. Rev.*, **2013**, *42*, 548.
[242] D. Taylor, S.J. Dalgarno, Z. Xu, F. Vilela, *Chem. Soc. Rev.*, **2020**, *49*, 3981–4042.
[243] J.X. Jiang, Y. Li, X. Wu, J. Xiao, D.J. Adams, A.I. Cooper, *Macromolecules.*, **2013**, *46*, 8779–8783.
[244] P. Pachfule, A. Acharjya, J. Roeser, T. Langenhahn, M. Schwarze, R. Schomäcker, A. Thomas, J. Schmidt, *J. Am. Chem. Soc.*, **2018**, *140*, 1423–1427.
[245] X. Li, Y.C. Zhang, Y. Zhao, H.P. Zhao, B. Zhang, T. Cai, *Macromolecules.*, **2020**, *53*, 1550–1556.
[246] S. Dadashi-Silab, F. Lorandi, M.J. DiTucci, M. Sun, G. Szczepaniak, T. Liu, K. Matyjaszewski, *J. Am. Chem. Soc.*, **2021**, *143*, 9630–9638.
[247] W.F. Wei, X. Li, K. Jiang, B. Zhang, X. Zhuang, T. Cai, *Angew. Chemie Int. Ed.*, **2023**, e202304608.
[248] P. Pachfule, A. Acharjya, J. Roeser, R.P. Sivasankaran, M.Y. Ye, A. Brückner, J. Schmidt, A. Thomas, *Chem. Sci.*, **2019**, *10*, 8316–8322.
[249] X. Fu, Z. Lu, H. Yang, X. Yin, L. Xiao, L. Hou, *J. Polym. Sci.*, **2021**, *59*, 2036–2044.
[250] Z. Lu, H. Yang, X. Fu, Y. Zhao, Q. Lin, L. Xiao, L. Hou, *Mater. Today Chem.*, **2022**, *25*, 100959.
[251] H. Yang, R. Zhao, Z. Lu, L. Xiao, L. Hou, *ACS Catal.*, **2023**, *13*, 2948–2956.
[252] R.Y. Liu, S. Guo, S.X.L. Luo, T.M. Swager, *Nat. Commun.*, **2022**, *13*, 1–8.
[253] J. Byun, Y. Hong, K.A.I. Zhang, *Chem Catal.*, **2021**, *1*, 771–781.
[254] X. Li, X.J. Zhang, W.L. Guo, Y. Huang, T. Cai, *Chem. Eng. J.*, **2023**, *465*, 142861.
[255] Y.W. Duan, X.J. Zhang, W.L. Guo, M. Jian, T. Cai, X. Li, *J. Mater. Chem. A.*, **2023**, *11*, 4639–4650.
[256] W.F. Wei, W.L. Guo, M. Jian, L.S. Qin, X. Li, T. Cai, *Chem. Eng. J.*, **2023**, *455*, 140631.
[257] H.C.J. Zhou, S. Kitagawa, *Chem. Soc. Rev.*, **2014**, *43*, 5415–5418.
[258] Y. Liu, B. Li, H.S. Li, P. Wu, J. Wang, *Dalt. Trans.*, **2020**, *49*, 17520–17526.
[259] T. Ma, K. Li, J. Hu, Y. Xin, J. Cao, J. He, Z. Xu, *Inorg. Chem.*, **2022**, *61*, 14352–14360.
[260] L. Zhao, Z. Du, G. Ji, Y. Wang, W. Cai, C. He, C. Duan, *Inorg. Chem.*, **2021**,.
[261] Y. Liu, C.T. Buru, A.J. Howarth, J.J. Mahle, J.H. Buchanan, J.B. Decoste, J.T. Hupp, O.K. Farha, *J. Mater. Chem. A.*, **2016**, *4*, 13809–13813.
[262] F.P. Kinik, A. Ortega-Guerrero, F.M. Ebrahim, C.P. Ireland, O. Kadioglu, A. Mace, M. Asgari, B. Smit, *ACS Appl. Mater. Interfaces.*, **2021**, *13*, 57118–57131.
[263] Q. Wang, Q. Gao, A.M. Al-Enizi, A. Nafady, S. Ma, *Inorg. Chem. Front.*, **2020**, *7*, 300–339.

[264] L. Zhao, Z. Du, G. Ji, Y. Wang, W. Cai, C. He, C. Duan, *Inorg. Chem.*, **2021**, *03*, 32.
[265] W. Liang, H. Chevreau, F. Ragon, P.D. Southon, V.K. Peterson, D.M. D'Alessandro, *CrystEngComm.*, **2014**, *16*, 6530–6533.
[266] Q. Xiong, Y. Chen, D. Yang, K. Wang, Y. Wang, J. Yang, L. Li, J. Li, *Mater. Chem. Front.*, **2022**, *6*, 2944–2967.
[267] M. Zhang, W. Zhou, T. Pham, K.A. Forrest, W. Liu, Y. He, H. Wu, T. Yildirim, B. Chen, B. Space, Y. Pan, M.J. Zaworotko, J. Bai, *Angew. Chemie.*, **2017**, *129*, 11584–11588.
[268] L. Shen, S. Liang, W. Wu, R. Liang, L. Wu, *Dalt. Trans.*, **2013**, *42*, 13649–13657.
[269] T.A. Goetjen, J. Liu, Y. Wu, J. Sui, X. Zhang, J.T. Hupp, O.K. Farha, *Chem. Commun.*, **2020**, *56*, 10409–10418.
[270] S. Mochizuki, T. Kitao, T. Uemura, *Chem. Commun.*, **2018**, *54*, 11843–11856.
[271] B.V.K.J. Schmidt, *Macromol. Rapid Commun.*, **2020**, *41*, 1900333.
[272] J. Zhang, F. Dumur, P. Horcajada, C. Livage, P. Xiao, J.P. Fouassier, D. Gigmes, J. Lalevée, *Macromol. Chem. Phys.*, **2016**, *217*, 2534–2540.
[273] H.L. Nguyen, F. Gándara, H. Furukawa, T.L.H. Doan, K.E. Cordova, O.M. Yaghi, *J. Am. Chem. Soc.*, **2016**, *138*, 4330–4333.
[274] B. Ohtani, O.O. Prieto-Mahaney, D. Li, R. Abe, n.d.
[275] H.L. Nguyen, T.T. Vu, D. Le, T.L.H. Doan, V.Q. Nguyen, N.T.S. Phan, *ACS Catal.*, **2017**, *7*, 338–342.
[276] T. Uemura, S. Horike, K. Kitagawa, M. Mizuno, K. Endo, S. Bracco, A. Comotti, P. Sozzani, M. Nagaoka, S. Kitagawa, *J. Am. Chem. Soc.*, **2008**, *130*, 6781–6788.
[277] C.S. Reddy, A. Arinstein, E. Zussman, *Polym. Chem.*, **2011**, *2*, 835–839.
[278] H. Xing, D. Chen, X. Li, Y. Liu, C. Wang, Z. Su, *RSC Adv.*, **2016**, *6*, 66444–66450.
[279] T. Uemura, Y. Ono, Y. Hijikata, S. Kitagawa, *J. Am. Chem. Soc.*, **2010**, *132*, 4917–4924.
[280] T. Uemura, Y. Ono, K. Kitagawa, S. Kitagawa, *Macromolecules.*, **2008**, *41*, 87–94.
[281] L. Zhang, X. Shi, Z. Zhang, R.P. Kuchel, R. Namivandi-Zangeneh, N. Corrigan, K. Jung, K. Liang, C. Boyer, *Angew. Chemie Int. Ed.*, **2021**, *60*, 5489–5496.
[282] Y. Huang, X. Li, Y.C. Zhang, Z. Shi, L. Zeng, J. Xie, Y. Du, D. Lu, Z. Hu, T. Cai, Z. Luo, *ACS Appl. Mater. Interfaces.*, **2021**, *13*, 44488–44496.
[283] L. Zhang, G. Ng, N. Kapoor-Kaushik, X. Shi, N. Corrigan, R. Webster, K. Jung, C. Boyer, L. Zhang, G. Ng, X. Shi, N. Corrigan, K. Jung, C. Boyer, N. Kapoor-Kaushik, R. Webster, *Angew. Chemie Int. Ed.*, **2021**, *60*, 22664–22671.
[284] X. Li, Y. Huang, W.F. Wei, W.L. Guo, Z. Luo, J. Xu, T. Cai, *Chem. Eng. J.*, **2022**, *434*, 134692.
[285] Y. Huang, W.L. Guo, J. Cheng He, X. Li, T. Cai, Y. Huang, W.L. Guo, J.C. He, X. Li, T. Cai, *Macromol. Rapid Commun.*, **2022**, *43*, 2200020.
[286] Z. Xia, B. Shi, W. Zhu, Y. Xiao, C. Lü, *Adv. Funct. Mater.*, **2022**, *32*, 2207655.
[287] C. Ponti, G. Nasti, D. Di Girolamo, I. Cantone, F.A. Alharthi, A. Abate, *Trends Ecol. Evol.*, **2022**, *37*, 281–283.
[288] K.A.S. Usman, J.W. Maina, S. Seyedin, M.T. Conato, L.M. Payawan, L.F. Dumée, J.M. Razal, *NPG Asia Mater.*, **2020**, *12*, 1–18.
[289] A. Elhage, B. Wang, N. Marina, M.L. Marin, M. Cruz, A.E. Lanterna, J.C. Scaiano, *Chem. Sci.*, **2018**, *9*, 6844–6852.
[290] R.I. Teixeira, N.C. De Lucas, S.J. Garden, A.E. Lanterna, J.C. Scaiano, *Catal. Sci. Technol.*, **2020**, *10*, 1273–1280.
[291] S.W. Lee, S. Obregón-Alfaro, V. Rodríguez-González, *J. Photochem. Photobiol. A Chem.*, **2011**, *221*, 71–76.
[292] H. O'Neal Tugaoen, S. Garcia-Segura, K. Hristovski, P. Westerhoff, *Sci. Total Environ.*, **2018**, *613–614*, 1331–1338.
[293] S. Zhang, J. Zhang, J. Sun, Z. Tang, *Chem. Eng. Process. - Process Intensif.*, **2020**, *147*, 107746.
[294] M.E. Fabiyi, R.L. Skelton, *J. Photochem. Photobiol. A Chem.*, **2000**, *132*, 121–128.
[295] A. Sridhar, R. Rangasamy, M. Selvaraj, *New J. Chem.*, **2019**, *43*, 17974–17979.
[296] Y. Chu, Z. Huang, R. Liu, C. Boyer, J. Xu, *ChemPhotoChem.*, **2020**, *4*, 5201–5208.
[297] R.G. Acres, A. V. Ellis, J. Alvino, C.E. Lenahan, D.A. Khodakov, G.F. Metha, G.G. Andersson, *J. Phys. Chem. C.*, **2012**, *116*, 6289–6297.
[298] J. Zhao, Y. Li, H. Guo, L. Gao, *Chinese J. Anal. Chem.*, **2006**, *34*, 1235–1238.
[299] L. Zheng, H. Xue, W.K. Wong, H. Cao, J. Wu, S.A. Khan, *React. Chem. Eng.*, **2020**, *5*, 1058–1063.
[300] C. McCullagh, N. Skillen, M. Adams, P.K.J. Robertson, *J. Chem. Technol. Biotechnol.*, **2011**, *86*, 1002–1017.
[301] A. Ying Shan, T. Idaty Mohd Ghazi, S. Abdul Rashid, *Appl. Catal. A Gen.*, **2010**, *389*, 1–8.
[302] F.L. Toma, L.M. Berger, D. Jacquet, D. Wicky, I. Villaluenga, Y.R. de Miguel, J.S. Lindeløv, *Surf. Coatings Technol.*, **2009**, *203*, 2150–2156.
[303] G. Li Puma, A. Bono, D. Krishnaiah, J.G. Collin, *J. Hazard. Mater.*, **2008**, *157*, 209–219.
[304] S.W. Verbruggen, S. Ribbens, T. Tytgat, B. Hauchecorne, M. Smits, V. Meynen, P. Cool, J.A. Martens, S. Lenaerts, *Chem. Eng. J.*, **2011**, *174*, 318–325.
[305] S. Shanmugam, S. Xu, N.N.M. Adnan, C. Boyer, *Macromolecules.*, **2018**, *51*, 779–790.
[306] K. Bell, S. Freeburne, M. Fromel, H.J. Oh, C.W. Pester, *J. Polym. Sci.*, **2021**, *59*, 2844–2853.
[307] G.J. Barbante, T.D. Ashton, E.H. Doeven, F.M. Pfeffer, D.J.D. Wilson, L.C. Henderson, P.S. Francis, *ChemCatChem.*, **2015**, *7*, 1655–1658.
[308] K. Bell, S. Freeburne, A. Wolford, C.W. Pester, *Polym. Chem.*, **2022**, *116*, 6120.
[309] K. Bell, S. Freeburne, M. Fromel, H.J. Oh, C.W. Pester, *J. Polym. Sci.*, **2021**, *59*, 2844–2853.
[310] X. Jiang, B. Wang, C.Y. Li, B. Zhao, *J. Polym. Sci. Part A Polym. Chem.*, **2009**, *47*, 2853–2870.
[311] K. Bell, Y. Guo, S. Barker, S.H. Kim, C.W. Pester, *Polym. Chem.*, **2023**, *14*, 2662–2669.
[312] M.C. Brochier Salon, P.A. Bayle, M. Abdelmouleh, S. Boufi, M.N. Belgacem, *Colloids Surfaces A Physicochem. Eng. Asp.*, **2008**, *312*, 83–91.
[313] M.B. Perez, M. Cirelli, S. de Beer, *ACS Appl. Polym. Mater.*, **2020**, *2*, 3039–3043.
[314] S. Minko, *J. Macromol. Sci. Part C Polym. Rev.*, **2006**, *46*, 397–420.
[315] A.C. Marques, M. Vale, D. Vicente, M. Schreck, E. Tervoort, M. Niederberger, *Glob. Challenges.*, **2021**, *5*, 2000116.
[316] M. Yaghmaei, A.E. Lanterna, J.C. Scaiano, *IScience.*, **2021**, *24*,.

[317] A. Elhage, B. Wang, N. Marina, M.L. Marin, M. Cruz, A.E. Lanterna, J.C. Scaiano, *Chem. Sci.*, **2018**, *9*, 6844–6852.
[318] W.L. Guo, Y. Zhou, B. Duan, W.F. Wei, C. Chen, X. Li, T. Cai, *Chem. Eng. J.*, **2022**, *429*, 132120.
[319] X. Li, Y. Li, Y. Huang, T. Zhang, Y. Liu, B. Yang, C. He, X. Zhou, J. Zhang, *Green Chem.*, **2017**, *19*, 2925–2930.
[320] Y. Wang, H. Li, J. Dong, L. Hu, D. Wei, L. Bai, H. Yang, H. Chen, *Macromol. Chem. Phys.*, **2021**, *222*, 2000406.
[321] A. Melker, B.P. Fors, C.J. Hawker, J.E. Poelma, *J. Polym. Sci. Part A Polym. Chem.*, **2015**, *53*, 2693–2698.
[322] M. Chen, J.A. Johnson, *Chem. Commun.*, **2015**, *51*, 6742–6745.
[323] M.H. Reis, F.A. Leibfarth, L.M. Pitet, *ACS Macro Lett.*, **2020**, *9*, 123–133.

Entry for the Table of Contents

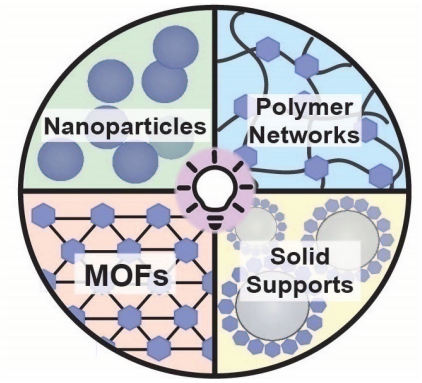

Heterogeneous photocatalysis can increase the sustainability of photochemistry by providing simple means for catalyst recovery and reuse. This review explores four prevalent classes of these materials: photocatalytic nanoparticles, polymer networks, metal organic frameworks (MOFs), and immobilized photocatalysts on solid supports in their use for light-mediate reversible deactivation radical polymerization.

Institute and/or researcher Twitter usernames: The Pennsylvania State University, @PesterGroup